


Spring 2018

Effects of Radiation on Neurite Morphology and Cytoskeleton Structure

Melissa Sassman
University of Southern Maine

Follow this and additional works at: <https://digitalcommons.usm.maine.edu/bio-students>

 Part of the [Astrophysics and Astronomy Commons](#), [Biology Commons](#), [Cellular and Molecular Physiology Commons](#), and the [Toxicology Commons](#)

Recommended Citation

Sassman, Melissa, "Effects of Radiation on Neurite Morphology and Cytoskeleton Structure" (2018). *Student Scholarship*. 2.
<https://digitalcommons.usm.maine.edu/bio-students/2>

This USM Access Thesis is brought to you for free and open access by the Biological Sciences at USM Digital Commons. It has been accepted for inclusion in Student Scholarship by an authorized administrator of USM Digital Commons. For more information, please contact jessica.c.hovey@maine.edu.

Effects of Radiation on Neurite Morphology and Cytoskeleton Structure

A THESIS SUBMITTED IN PARTIAL FULFILLMENT OF THE
REQUIREMENTS FOR THE DEGREE OF MASTER OF SCIENCE IN BIOLOGY
UNIVERSITY OF SOUTHERN MAINE
DEPARTMENT OF BIOLOGICAL SCIENCES

MELISSA SASSMAN

June 2nd, 2017

**THE UNIVERSITY OF SOUTHERN MAINE
DEPARTMENT OF BIOLOGICAL SCIENCES**

Date: June 2nd, 2017

We hereby recommend that the thesis of Melissa Sassman entitled:

Effects of Radiation on Neurite Morphology and Cytoskeleton Structure

Be accepted as partial fulfillment of the requirements for the degree of

Master of Science in Biology

Signatures



Melissa Sassman

Date: 10/17/17

Advisory Committee:



Douglas Currie, Graduate Advisor

Date: 10/17/17



David Champlin

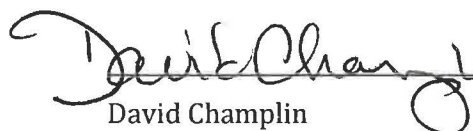
Date: 10/17/17



Rachel Larsen

Date: 10/17/17

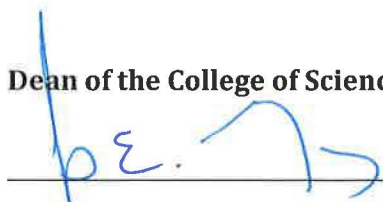
Chair of the Department of Biological Sciences



David Champlin

Date: 10/17/17

Dean of the College of Science, Technology and Health



James E. Graves

Date: 10/17/17

AKNOWLEDGEMENTS

Foremost, I'd like to express my deep gratitude to my advisor Dr. Doug Currie for all of his guidance and encouragement throughout the process of this master thesis.

Mostly, I'd like to thank him for allowing me the time and space, without judgement, to be what I believe is one of the most essential components of a scientist-curious.

I'd also like to thank the rest of my thesis committee, Dr. David Champlin for being a proliferator of good vibes and for continued understanding and support, and Dr. Rachel Larsen for her insight and challenging me to think critically.

Lastly, I'd like to thank my family, friends, and especially my husband Lucas for continued support and reassurance throughout this journey. It wouldn't have been possible without you.

ABSTRACT

Long-term manned space exploration to the moon, Mars, and other areas beyond Earth's protective magnetic field poses possible acute and late central nervous systems (CNS) risks. Of particular concern for astronauts is exposure to high atomic number, high energy particles known as HZE particles, a component of galactic cosmic radiation (GCR). Although NASA has radiation safety requirements, the possible effects of GCR and HZE particles on the central nervous systems of astronauts remains unknown. Understanding the risks and effects of galactic cosmic radiation and HZE particles on the central nervous system will allow for safer space exploration.

Additionally, and perhaps more relevant, are the effects on the CNS of patients undergoing radiation therapy for cancer treatment or for medical procedures like CT scans. Radiation (using x-rays, gamma rays, and charged particles), along with chemotherapy, is widely used to treat primary and metastatic brain tumors. Despite advances in radiation therapy, significant negative impacts on the CNS still remain.

In this study, our aim was to understand the effects of x-ray radiation on neurite morphology and cytoskeleton structure using human SH-SY5Y cells, a neuroblastoma cell line commonly used for neurite outgrowth studies. In addition, we monitored cytotoxicity via a metabolic proliferation assay in neuronal cells lines, as well as a primary glial cell line and glial cell line derived from a glioma.

Immunocytochemistry results suggests that neurite length of differentiated SH-SY5Y cells decreases with increases in radiation dose and exposure time. Phase contrast microscopy results are contradictory; suggesting no significant differences between treated and control groups with regards to dose and time. Phase contrast microscopy does reveal neurite complexity decreases in differentiated SH-SY5Y cells with select dosages and times of exposure.

Cytotoxicity results are wildly disparate between cells lines. Data indicate radiation dose and time post-treatment affect metabolic activity. However, metabolic activity between cell lines and within a cell line can either increase or decrease in response to dose and time.

TABLE OF CONTENTS

LIST OF TABLES	viii
LIST OF FIGURES	ix
1: INTRODUCTION	1-30
1.1 Radiation	1
1.1.1 What is Radiation?	1
1.1.2 Sources of Radiation	1
1.1.3 Types of Radiation	2
1.1.3.1 Non-Ionizing	2
1.1.3.2 Ionizing	3
1.1.4 How is Radiation Measured?	5
1.1.5 Why is Ionizing Radiation Harmful?	8
1.2 NASA's Concern	8
1.2.1 Solar Particle Events	8
1.2.2 Galactic Cosmic Radiation	10
1.3 Central Nervous System & Neuronal Development	10
1.3.1 Cells of the Central Nervous System	11
1.3.2 Cytoskeleton Components & Dynamics	13
1.4 Biological Effects of Ionizing Radiation	15
1.4.1 Molecular Effects	16
1.4.2 Evidence from Cell & Tissue Models	21
1.4.3 Evidence from Animal Behavior Studies	24
1.4.4 Evidence from Human Data	25
1.4.5 Combating Effects of Radiation	26
1.5 Radiation Therapy	27
1.6 Our Focus	28
2: MATERIALS & METHODS	30-40
2.1 Cell Culture	30
2.1.1 SH-SY5Y Cell Line	30
2.1.2 C6 Cell Line	31
2.1.3 CL-mPG-15 Cell Line	31
2.2 Preliminary Experiments	32
2.3 Treatment	33
2.4 Phase Contrast Microscopy	34
2.5 Immunocytochemistry	35
2.5.1 Cytoskeleton Staining of SH-SY5Y Cells	35
2.5.2 GFAP Staining of Primary Glial Cell Line	37
2.6 MTS Assay	38

3: RESULTS	40-74
3.1 Preliminary Experiments (density & dose testing)	40
3.2 Effects of Radiation on Differentiated SH-SY5Y Morphology	41
3.3 Effects of Radiation on SH-SY5Y Cytoskeleton Structure	43
3.4 Cytotoxicity of Radiation	44
3.4.1 MTS Assay of SH-SY5Y Cell Line	44
3.4.2 MTS Assay of C6 Cell Line	45
3.4.3 MTS Assay of CL-mPG-15 Cell Line	45
3.5 Figures	47
4: DISCUSSION	75-88
4.1 General	75
4.1.1 Preliminary Experiments (seeding density and dose testing)	75
4.1.2 Effects of Radiation on Differentiated SH-SY5Y Morphology	76
4.1.3 Effects of Radiation on SH-SY5Y Cytoskeleton Structure	77
4.1.4 Cytotoxicity of Radiation	80
4.2 Future Aims	84
4.2.1 General	84
4.2.2 Reducing Effects of Radiation	85
4.2.2.1 Nutraceuticals	85
4.2.2.2 Erythropoietin (EPO)	86
5: CONCLUSION	87-88
6: REFERENCES	88-104

LIST OF TABLES

Table 1	Seeding densities for each cell line and assay performed	56
---------	--	----

LIST OF FIGURES

Figure 1	Images used to determine appropriate seeding density of SH-SY5Y cell line	52
Figure 2	Metabolic curve for SH-SY5Y cell line	53
Figure 3	Metabolic curve for C6 cell line	54
Figure 4	Metabolic curve for m-15 cell line	55
Figure 5	Preliminary x-ray radiation dose testing of SH-SY5Y cell line using MTS assay	57
Figure 6	Additional x-ray radiation dose testing of C6 cell line	58
Figure 7	Additional x-ray radiation dose testing of m-15 cell line	59
Figure 8	Representative images of glial fibrillary acidic protein (GFAP) staining of m-15 cell line	60
Figure 9	Cell number decreases in differentiated SH-SY5Y cells 24 and 48 hours post-treatment in response to increased x-ray radiation dose according to phase microscopy	61
Figure 10	Neurite length does not change with increases in both dose and time post-treatment based on phase contrast microscopy	62
Figure 11	Number of branch points decrease in differentiated SH-SY5Y cells in select dose and time groups according to phase microscopy	63
Figure 12	Representative images of immunocytochemistry staining for SH-SY5Y cell line	64
Figure 13	Neurite length of differentiated SH-SY5Y cells decreases in response to increased radiation dose and time post-treatment based on immunocytochemistry	65
Figure 14	Control cells 48 hours post-treatment tend to exhibit complicated cytoskeleton structure	66
Figure 15	Treated SH-SY5Y cells possess the same overall cytoskeleton structure seen in control cells, although they tend to be shortened and less complex	67
Figure 16	Not all control cells exhibit complex networking	68

LIST OF FIGURES, continued

Figure 17	Treated SH-SY5Y cells can display complex neurites	69
Figure 18	Number of collapsed growth cones does not change with dose or time (post-treatment) between SH-SY5Y control cells and x-ray treated cells	70
Figure 19	X-ray radiation causes a decrease in metabolic activity in SH-SY5Y cell line as determined by MTS assay	71
Figure 20	X-ray radiation causes an increase in metabolic activity 48 hours post-treatment in the C6 cell line as determined by the MTS assay	72
Figure 21	X-ray radiation causes an increase in metabolic activity in the m-15 cell line as determined by the MTS assay	73

1: INTRODUCTION

1.1 RADIATION

1.1.1 WHAT IS RADIATION?

Radiation is the emission or transmission of energy in the form of rays, electromagnetic (EM) waves, or high-speed subatomic particles. While humans and other animals can see or feel some forms of radiation, other forms can only be detected using specialized equipment. Electromagnetic radiation can act as both waves and streams of particles. Known as photons, these particles have no mass. The full range of photon energies and their corresponding wavelengths is known as the electromagnetic spectrum. Photons with higher energy exhibit shorter wavelengths while, conversely, those with lower energies have longer wavelengths. It is well known that as the energy of the radiation increases (and wavelength shortens) so does the probability of biological harm (Rask, J. et al. 2007).

1.1.2 SOURCES OF RADIATION

We are exposed to electromagnetic radiation constantly. Man-made technologies are a large contributor to EM radiation exposure and includes, but is not limited to, the use of microwaves, cell phones, light bulbs, heaters, gamma-ray sterilizers (which act to sterilize food), and diagnostic medical tools (like x-rays or CT scans). There are also naturally occurring sources of EM and ionizing radiation which includes radioactive elements within the Earth's crust, particles trapped within the VanAllen Belts (Earth's magnetic field), and astrophysical matter like stars.

However, the sun is the largest source of radiation. Although the sun emits all wavelengths in the electromagnetic spectrum, most are visible, infrared and ultraviolet radiation (UV) in origin. However, the sun releases immense amounts of energy via solar flares and coronal mass ejections (CME), emitting x-rays, gamma rays, and solar particle events (SPE)-streams of protons and electrons. It is these solar particle events, along with galactic cosmic radiation, that are of concern to the National Aeronautics and Space Administration (NASA) and astronauts that travel beyond low-Earth orbit (Rask, J. et al. 2007).

1.1.3 TYPES OF RADIATION

1.1.3.1 Non-Ionizing Radiation

Radiation can be classified as either non-ionizing or ionizing. Non-ionizing radiation (NIR) is an electromagnetic radiation that does not have enough energy to cause ionization of atoms or molecules as it passes through matter. Instead, there is only enough energy to cause excitation of electrons. On the electromagnetic spectrum, non-ionizing radiation is fairly low-energy with longer wavelengths, low frequency, and low photon energy (the speed or energy at which rays travel). The NIR spectrum is divided into two regions, optical radiation and electromagnetic fields (EMFs). Optical radiation is simply emitted light and includes ultraviolet (UV), visible, and infrared radiation. The greatest risks from optical radiation are probably due to UV radiation emitted by the sun. Skin exposure can cause redness and burning, accelerated aging, and increased risk of skin cancer. Exposure of eyes to UV light can cause cornea and retina damage and increases the risk of cataracts.

Electromagnetic fields arise from electrically charged particles and include extremely low frequency (ELF), radio frequency, and microwaves. Sources of EMFs include microwaves, power lines, wireless networks, cell phones, and many others. Despite the fear that EMFs cause cancer, the National Research Council (NRC) found that "no conclusive and consistent evidence" exists that EMFs cause harm to humans. Additionally, the International Agency for Research on Cancer (IARC) found that ELF magnetic fields are *possible* human carcinogens due to limited or inadequate evidence for carcinogenicity and radio EMFs are *possible* human carcinogens based on limited evidence in human and animal studies (IARC Working Group on the Evaluation of Carcinogenic Risks to Humans, World Health Organization, & International Agency for Research on Cancer 2002, 2013). Acute exposures to electromagnetic fields may cause heating of biological tissues, but are generally thought to be harmless (Park 2001).

1.1.3.2 Ionizing Radiation

Ionizing radiation (IR) is classified as either electromagnetic or particulate in nature. IR carries enough energy to cause removal or liberation of electrons from atoms as it traverses matter - thereby causing ionization. Ionizing radiation includes the high energy portion of the electromagnetic spectrum with shorter wavelengths and higher frequencies. Electromagnetic IR consists of photons, discrete bundles of electromagnetic (light) energy that have neither mass nor charge. Ionizing radiation includes x-rays, gamma rays, alpha particles, beta particles, and galactic cosmic

radiation (GCR). Although they are similar, x-rays and gamma-rays differ in source of origin, frequency, wavelength, and photon energy. Gamma-rays are higher in energy and originate from the nucleus, usually as a product of radioactive decay. X-rays arise outside the nucleus as electrons transition between orbitals.

Particulate radiation consists of atomic or subatomic particles carrying kinetic energy. Included in ionizing particle radiation are alpha (α) particles, beta (β) particles, and neutrons. Alpha and beta particles are directly ionizing because they carry a charge and can interact with atomic electrons through coulombic forces. Alpha particles are subatomic fragments consisting of two protons and two neutrons expelled from the nuclei of unstable atoms. They are typically produced in the process of alpha decay. Because they have two protons and two neutrons they are identical to a helium nucleus and often referred to as He^{2+} . They are relatively heavy, high-energy, charged particles, and because of this travel fairly slowly (about one-twentieth the speed of light). Alpha particles are not radioactive and gain free electrons once their energy is depleted thus becoming helium. Due to the fact that they lose energy quickly, alpha particles cannot penetrate most matter and therefore do not pose a health risk to humans. However, individuals may be at a greater risk of cancer if alpha emitters are ingested, absorbed into the bloodstream, or inhaled. Radon gas is the largest natural source of alpha particle radiation to the general population <http://www.epa.gov/radiation/understand/alpha.html>.

Beta decay exists in two forms, β^- and β^+ , which give rise to electrons or positrons, respectively. Beta decay is a type of radioactive decay responsible for the production of beta particles. Unlike alpha particles, beta particles are high in both energy and speed and have a mass of zero. Collectively, this gives them more penetrating ability and consequently causes more cell damage. Internal exposures to beta emitters causes increased risk of cancer. Although individuals can be exposed to natural beta decay, much of the exposure is man-made. Sources include medical imaging (magnetic resonance imaging, MRI), industrial instruments (thickness gauges), and use of radioactive materials to diagnose and treat medical conditions (such as the case with radioactive iodine).

Neutrons are subatomic particles that, with protons, make up the nucleus of an atom. Neutrons have no charge and therefore cannot directly ionize an atom. Instead they are indirectly ionizing. A stable atom can become unstable once it absorbs a neutron which in turn can cause emission of ionizing radiation. For this reason, neutrons are considered the only type of radiation that causes radioactivity in other materials (Hall and Giaccia 2012).

<https://www.mirion.com/introduction-to-radiation-safety/types-of-ionizing-radiation/>

1.1.4 HOW IS RADIATION MEASURED?

The absorbed dose of radiation is defined as the amount of energy deposited by radiation per unit mass of material. It can be expressed as units of rad (radiation

absorbed dose), Grays is the international unit (1 Gray = 1 Gy = 1 Joule of energy per kilogram of material = 100 rad), or mGy (milliGray) which describes how much radiation is absorbed by the body. Due to the fact that equal doses of differing ionizing radiation types can cause very different biological damage, an equivalent dose unit is used. Because of this, the equivalent dose describes both the amount of radiation absorbed as well as the amount of damage a particular radiation type causes. Equivalent dose is measured in Sieverts (Sv) or milliSieverts (mSv) (Rask, J. et al. 2007).

It is estimated that astronauts who are at an international space station receive approximately 80 and 160 mSv of radiation during solar maximums and minimums, respectively. To put that into perspective, one mSv of space radiation is roughly the same dose as three chest x-rays, despite differences in types of radiation (NASA, 2002). Crew members aboard the space station wear dosimeters and also have biodosimetry evaluations which measures chromosomal damage in red blood cells due to radiation exposure. Additionally, radiation measurement devices and various experiments have flown or been placed by various agencies outside and within the International Space Station (ISS). These include but are not limited to: Passive Dosimetry (1999-present), Bonner Ball Neutron Detector (March-December 2001), Charged Particle Directional Spectrometers (CPDS)(2001-present), Dosimetric Mapping (DOSMAP)(March-August 2001), and Phantom Torso (March-August 2001) (NASA, 2002). However, these are measurements and estimates at the ISS and

therefore not applicable to quality and quantity of radiation outside low-Earth orbit (LEO).

According to the National Council of Radiation Protection and Measurements (NCRP, 2006), it is estimated that astronauts traveling outside Earth's protective magnetic field may receive radiation doses two times that of levels found in LEO. Earth's magnetic field is believed to be due to its liquid outer core. Comprised of metal, this liquid outer core flows as a result of convection as well as Earth's rotation. This flow of the liquid outer core generates electrical currents which gives rise to magnetic fields.

Until recently, reliable dosimetry data for total dose, dose rate, and radiation quality encountered in space was relatively unknown. Past estimates relied on inferring about space radiation from data collected on Earth. Unmanned space crafts and mathematical models have made it possible to accurately estimate GCR dose-rates. These models include *Nymmik's Model*, *CREME-96 Model*, *CHIME Model*, and *Badhwar and O'Neill Model* (NCRP, 2006). A Radiation Assessment Detector (RAD) attached to the Mars Curiosity rover was carried by the Mars Science Laboratory (MSL-RAD) in order to gain estimates of primary and secondary particles (Chancellor et al. 2014; Zeitlin et al. 2013; Kim, M.-H. Y., et al. 2014). The Mars radiation environment experiment (MARIE) is still in use today and measures both the amount and types of radiation experienced in transit to Mars as well as on the planet itself (NASA, 2002). Comparisons of data collected from the NASA Space

Cancer Risk Model (NSCR-2012) and MSL-RAD show a consistency in measurements of GCR dose rates. Therefore, we can reasonably assume accurate estimates of GCR doses encountered beyond LEO ([Cucinotta et al. 2001](#); [Cucinotta et al. 2011](#)).

Other studies have aimed at providing cell-hit frequencies experienced by astronauts outside the magnetosphere. Using two different shielding configurations, Curtis and Letaw (1989) provide evidence that astronauts on a three-year mission in a most heavily shielded spacecraft would have 33% of cell nuclei traversed by particles with a charge between 3 and 28. Approximately 6% of cell nuclei would experience a second traversal. This study also found that increasing shielding could decrease the dose equivalent by a factor of 3 via decreasing both the absorbed dose and biological effectiveness ([Chancellor et al. 2014](#); [Curtis, 1989](#)).

Individual risk factors can compound risk estimates. Potential CNS detriment to astronauts is not only a function of radiation quality and quantity, but also age, genetic predisposition, sex, previous radiation exposure, and prior head injuries. Synergistic effects between GCR exposure and effects of space travel on the CNS are also plausible since microgravity, sleep deprivation due to disruption in circadian rhythm, and isolation/confinement can affect the CNS ([Cucinotta et al. 2014](#)).

1.1.5 WHY IS IONIZING RADIATION SO HARMFUL?

Although non-ionizing radiation does cause biological harm, we are able to efficiently shield against it. Ionizing radiation, however, is hard to avoid due not only to its ability to penetrate matter but also by its ability to alter matter (ionization) as

it passes through. It has been described as an “atomic-scale cannonball” as it breaks through matter causing substantial damage in its wake (Rask, J. et al. 2007).

Additional damage can be caused by secondary particles. Interaction of primary particles, like GCR, can interact with spacecraft material or biological tissue giving rise to secondary particles, an added concern of NASA (Chancellor et al. 2014; Cucinotta et al. 2014; Cucinotta and Durante 2006; Curtis 1989; Held 2009; Sridharan et al. 2015).

1.2 NASA’s CONCERN

Long-term manned space exploration to the moon, Mars, and other areas beyond Earth’s protective magnetic field pose health concerns to astronauts due to the unique nature of radiation encountered in space. Of particular concern for astronauts are acute exposures to sporadic solar particle event (SPE) and chronic exposures to galactic cosmic radiation (GCR). Although the Van Allen Belts are comprised of protons and electrons that are trapped in Earth’s magnetic field, they are likely small contributors to total space radiation exposure and therefore will not be discussed further (McKenna-Lawlor et al. 2012).

1.2.1 SOLAR PARTICLE EVENTS

Solar particle events (SPE) cause the release and/or acceleration of high energy protons and heavy ion particles into the interplanetary medium (Chancellor et al. 2014; McKenna-Lawlor et al. 2012;). Consequently, sudden large increases in radiation would occur both the exterior and interior of space crafts. The Sun’s

activity is based on an approximate 11-year solar cycle which is divided into periods of solar minimum (four inactive years) and solar maximum (seven active years). Increases in solar flares, sudden bursts of magnetic energy, or coronal mass ejections (CMEs), large explosions of magnetized plasma originating from the corona-the sun's outermost atmosphere, during solar maximums give rise to SPEs. Although SPEs are more likely to occur during solar maximums, they can occur at any time during the 11-year solar cycle thus making it impossible to predict the timing of a large SPE. Although each SPE varies in its particle composition they are mainly composed of protons, about 4% helium, and less than 1% of heavier ions (Wu et al. 2008). During an SPE, doses range from 0-100 mGy/h for those inside a space vehicle and from 0-500 mGy/h for astronauts performing extravehicular activity (EVA) (Chancellor et al. 2014). The majority of solar particle events are both low in intensity and have soft spectra (rapid decrease in particle fluence rate-number of particles crossing per unit time, with increase in energy) and consequently are not an exposure concern since the spacecraft itself provides shielding.

What is of concern are large SPEs that, within hours or days, could cause acute radiation syndrome (ARS) (National Council of Radiation Protection and Measurements, 2006; Wu et al. 2008). ARS is clinically classified as hematopoietic syndrome, GI syndrome, and neurovascular syndrome, prodromal effects (early symptoms) including nausea, vomiting, anorexia, and fatigue, as well as skin injuries, depletion of blood cells and blood-forming organs, and immune system

dysfunction ([Bevelacqua 2008](#); [Bruno and Czysz 2009](#); [Chancellor et al. 2014](#); [Wu et al. 2008](#)). Although it is known that both x-rays and gamma rays can cause ARS, the acute effects of exposure to SPE protons remains unknown. Extravehicular activity is a concern as shielding from the spacecraft is eliminated. Although shielding is one approach to abate the effects of SPE particles and galactic cosmic radiation, it is expensive and should not be overestimated ([Wu et al. 2008](#)).

1.2.2 GALACTIC COSMIC RADIATION

Galactic cosmic radiation, or galactic cosmic rays, come from outside the solar system, but mainly arise from within our Milky Way galaxy. GCR are atomic nuclei, their electrons removed as they travel through the galaxy at nearly the speed of light ([Chancellor et al. 2014](#)). GCR dose is highest at solar minimums due to the fact that particles are influenced by the Sun's magnetic field. During solar minimums, the magnetic field of the Sun is most weak and therefore less capable of deflecting particles ([Rask, J. et al. 2007](#)). Galactic cosmic radiation is mainly composed of energetic protons (hydrogen, ~85%) and alpha particles (helium nuclei, ~14%). Of greatest concern are the less abundant component of GCR, high atomic number, high energy particles known as HZE particles. Charges of HZE particles range from $Z=3$ to $Z=26$, or lithium and nickel, respectively. Iron is a transition metal with a charge of $Z=26$ and it, along with other ionized transition metals, are biologically harmful since they cannot be shielded against with any feasible amount of spacecraft material ([Rask, J. et al. 2007](#)). GCR particles have a large range of energies (~ 10 MeV/n to $\sim 10^{12}$ MeV/n) and because of this shielding is problematic. Consequently,

astronauts would be exposed to constant, low dose-rate radiation (National Council on Radiation Protection and Measurements, NCRP, 2006). GCR is extremely biologically harmful due to its high ionizing power, immense penetrating ability, and large potential for extensive radiation induced damage (Chancellor et al. 2014; Held 2009; Rask, J. et al. 2007). Additionally, shielding could cause adverse effects since particles are fragmented as they pass through spacecraft material giving rise to secondary particles which could cause greater biological harm (Chancellor et al. 2014; Held 2009).

1.3 CENTRAL NERVOUS SYSTEM & NEURONAL DEVELOPMENT

1.3.1 CELLS OF THE CENTRAL NERVOUS SYSTEM

The central nervous system (CNS) is mainly comprised of two types of cells, neurons and neuroglia. It is estimated that there are approximately 100 billion neurons in the human brain; which are able to process and transmit information via electrical and chemical signals. A neuron consists of three main parts- a cell body (or soma), axon, and dendrites. The cell body contains many organelles, including the nucleus. Extending from the soma are neurites, which collectively includes dendrites and axons. Dendrites branch from the soma and are the postsynaptic portion of the synapse, receiving chemical signals in the form of neurotransmitters from axons of other neurons. Dendrites serve to transmit the nerve impulse *to* the cell body. The axon is a long projection that extends from the soma at a site known as the axon hillock. Its purpose is to carry electrical impulses *away* from the cell body to other

neurons, muscles, or glands. Therefore, it is considered the presynaptic portion of the synapse.

Nearly 85% of the brain is comprised of glial cells. Glia, which comes from the Latin for glue, have historically been regarded as supporting cells for neurons. Two classes of glial cells exist, microglia and macroglia (Kandel et al. 2000).

Microglia are a type of immune cell found only in the brain, although they are derived from macrophages outside of the CNS. These phagocytic cells are activated upon injury, infection, or disease. Neurodegenerative diseases, such as Alzheimer's may also initiate microglial activation. Microglia are able to act as macrophages, detecting and engulfing damaged neurons, or portions of neurons, as well as viruses and bacteria (Kandel et al. 2000; Purves et al. 2001).

Macroglia consist of oligodendrocytes, astrocytes, and Schwann cells; although Schwann cells form sheaths around axons of peripheral nerves. Oligodendrocytes make up the myelin sheath-a protective covering that serves to expedite action potentials that travel through the axon (Kandel et al. 2000; Purves et al. 2001).

Astrocytes are star shaped and provide a variety of functions. Astrocytes not only provide support for neurons, but they also control the supply of nutrients and oxygen. Astrocytes have been found to release gliotransmitters and can modify signals that neurons both send and receive. Additionally, evidence suggests that

astrocytes may be involved in the growth and development of neurons and synapses along with the potential to signal immune cells to sites of damage. Collectively, this means astrocytes are capable of communicating with neurons and are much more important than once believed (Kandel et al. 2000; Purves et al. 2001; Raff et al. 1979; Sagara et al. 1993).

Until recently, the importance of glial cells has been largely ignored. More recently, glia have been discovered to be involved in diseases like brain cancer and multiple sclerosis. They have also been implicated in psychiatric illnesses, neurodegenerative disorders, chronic pain, infectious diseases, and repair of the CNS after injury.

Because of all this, and due to the important functions glial cells carry out, there is now an acceleration of glial research in order to better understand events that occur *in vivo*.

1.3.2 CYTOSKELETON COMPONENTS AND DYNAMICS

Pathfinding is the process in which neurons send out axons to their target cells or synaptic partners allowing the establishment of proper circuitry. A functional nervous system is one where neurons have successfully achieved pathfinding. Axon guidance is reliant on the growth cone, the ambulatory tip of growing axons, as well as extracellular cues (Geraldo and Gordon-Weeks 2009; Lowery and Van Vactor 2009). Growth cones are an integral feature of neurite outgrowth and interactions of growth cone cytoskeleton components are dynamic. The two major cytoskeletal filaments in neurons consist of actin and microtubules. Actin monomers make up

actin filaments-a polarized polymer whose plus (barbed) end faces the leading edge of the growth cone (or edge of growing P-domain) and minus (pointed) end faces the T-zone. Polymerization of ATP-actin typically occurs at the plus end, with ADP-actin depolymerization at the minus end. Microtubules (MT) are also polarized and are comprised of α - and β -tubulin dimer arrays. MT polymerization takes place at the plus end where GTP-tubulin dimers are added while MT depolymerization via GTP hydrolysis causes GDP-tubulin dimer dissociation at the minus end (Lowery and Van Vactor 2009; Vitriol and Zheng 2012).

Growth cones consist of three distinct domains. At the end of the neurite entering the growth cone lies the central domain, or C-domain. The C-domain consists of bundles of stable microtubules, as well as vesicles and organelles like mitochondria. The peripheral domain, or P-domain, is most distal and contains F-actin bundles which make up filopodia and an F-actin mesh that makes up lamellipodia-like veils. Between the C and P domains is the transition (T) zone where F-actin arcs (actomyosin contraction units) are arranged perpendicular to F-actin bundles forming a semicircular region (Lowery and Van Vactor 2009).

As the growth cone moves it constantly cycles through three observable stages termed, protrusion, engorgement, and consolidation (Dent and Gertler 2003; Goldberg and Burmeister 1986; Lowery and Van Vactor 2009). Protrusion starts when growth cone receptors bind an adhesive substrate. An intracellular cascade enables substrate and cytoskeleton to link. F-actin retrograde flow is halted while

polymerization at the plus end continues. Consequently, filopodia and lamellipodia extend. Exploratory microtubules invade the P-domain prior to protrusion and may act as guidance sensors. During engorgement however, the C-domain moves forward as stable microtubules continue to move into the P-domain where protrusion has occurred thus acting to steer the growth cone and fixing the direction of growth. Finally, the new portion of axon is formed when actin filaments in the wrist of the growth cone depolymerize causing consolidation of MTs (Lowery and Van Vactor 2009).

1.4 BIOLOGICAL EFFECTS OF IONIZING RADIATION

Although electromagnetic and subatomic particle radiations are both ionizing, they differ in the amount of energy they transfer per unit length to the materials they traverse. X-rays and gamma-rays are examples of low linear energy transfer (low-LET) radiation. Low-LET radiation is considered sparsely ionizing since only a few dozen ionizations are produced when fast electrons traverse a cell. Conversely, subatomic particle electromagnetic radiation is considered high-LET radiation and is densely ionizing. This is because they transfer more energy per unit length as they pass through matter and are therefore more damaging than low-LET (Held 2009; National Research Council, 2006). While astronauts will mostly be exposed to high-LET, treatment for this study will be done using low-LET for three reasons. Firstly, preliminary data it needed to gain time on particle accelerators that would provide high-LET. Secondly, time and money is limited and treatment with high-LET is currently beyond our reach. Lastly, there is a much higher incidence of people

exposed to low-LET in comparison to GCR due to radiation therapy for cancer patients and overuse of diagnostic medical tools like CT scans. For this reason, biological effects of both types of linear energy transfer radiations will be discussed. Concerns for possible CNS damage arose after the discovery of GCR by Cornelius Tobias who predicted the light flash phenomenon as a single HZE nuclei traverses the retina. This would later be confirmed by Apollo astronauts (Cucinotta et al. 2014). Both acute and late central nervous systems (CNS) risks from space radiation are concerns of NASA regarding space travel beyond LEO. Acute CNS risks include altered cognitive function, reduced motor function, and changes in behavior. Late CNS risks are dementia, premature aging, cancer, and neurodegenerative disorders such as Alzheimer's Disease (AD) (Cucinotta et al. 2009).

Although NASA has radiation safety requirements, the possible effects of GCR and HZE particles on the central nervous systems of astronauts remains unknown (Cucinotta et al. 2009). The NASA Chief Health and Medical Officer have set permissive exposure limits (PELs) for both cancer and non-cancer risks to blood forming organs (BFOs), skin, and eye lenses which have been in place since 1970. However, these PELs are for short term exposures or for career exposures of astronauts doing non-exploratory missions. Astronauts on previous NASA missions are not likely to exhibit observable CNS effects because their missions were short and they were afforded the protection of Earth's magnetic field; there are also few astronauts, creating a small population size. Such small sample sizes decrease confidence in results of radiation studies and make it difficult to estimate future

risk. For astronauts who will be exploring, preliminary exposure limits are limited and based on experimental animal studies. In order to improve our understanding of the biological effects of space radiation and set PELs for travel beyond LEO further studies need to verify CNS risks shown in recent investigations (Cucinotta et al. 2009).

1.4.1 MOLECULAR EFFECTS

Despite the fact that ionizing radiation causes ionization and therefore only interacts with atoms or molecules within the cell, it is these interactions that are the source of biological detriment. The disturbance of atoms and/or molecules can negatively impact cells which may ultimately affect tissues, organs, and the entire body (Little et al. 2010).

Radiation may affect cells via two mechanisms termed direct and indirect effects (U.S. Nuclear Regulatory Commission). Direct effects occur when an ionizing particle directly interacts with DNA. Direct effects may also affect other macromolecules like RNA, proteins, and enzymes however, damage to DNA is the primary concern since it is not only the most crucial macromolecule but also the most radiosensitive (Samari et al. 2013). DNA lesions caused by direct and indirect effects include base alterations, DNA-DNA and DNA-protein crosslinks, and both single and double strand breaks (Morgan et al. 1996). It is thought that upon exposure to IR, damage to cells caused by direct effects is dealt with rapidly by either tagging

macromolecules for degradation or by repairing DNA through various repair mechanisms.

Indirect effects begin with the interaction of ionizing particles and water molecules (since water makes up approximately 70% of human tissue) resulting in the ionized water molecule, H_2O^+ . Further reactions can produce hydrogen radicals ($H\bullet$), hydroxyl radicals ($OH\bullet$), and hydrogen peroxide (H_2O_2). Ultimately, the interaction of ionizing radiation and water results in reactive oxygen species (ROS) like those listed above, which can rapidly self-amplify and persist through interactions with lipids, membranes, and oxygen (National Research Council 2006; Barcellos-Hoff et al. 2005).

Increases in ROS upon exposure to radiation have been divided into three temporal categories, early which occurs within minutes, delayed occurring in hours, and chronic occurring in weeks or months. Initial spikes in ROS occur within 15-30 minutes of radiation exposure and can be attributed to NADPH oxidase activity. It is this early ROS response that is responsible for bystander effects (Sridharan et al. 2015). The bystander effect is considered a type of non-targeted effect (NTE) where responses to radiation can be seen in cells not subjected to radiation but were either adjacent or spatially separated by cells that were irradiated (Cucinotta and Chappell 2010; Morgan and Sowa 2007). There are two mechanisms in which bystander effects occur. Extracellular factors, like ROS, exosomes, and soluble signaling factors secreted by affected cells can cause biological responses in non-irradiated cells.

Additionally, signaling molecules can be transmitted through intercellular gap junctions resulting in damage amplification (Morgan and Sowa 2007; Sridharan et al. 2015).

Delayed responses, marked by a second surge of ROS, can be seen within 6-12 hours post exposure. It is likely this rise in ROS originates from mitochondria and may serve to promote cell death (Saenko et al. 2013; Sridharan et al. 2015; Yamamori et al. 2012).

Chronic ROS production can last for weeks, months, even years and persists in both irradiated and non-irradiated progeny. Type of damage is dependent on the tissue affected. For example, persistent ROS in the brain cortex has been associated with cell death, continual DNA damage response activation, arrest of cell growth, senescence, cell layer thinning, tissue volume reduction and reduced cognitive ability (Suman et al. 2013; Sridharan et al. 2015). Neurogenesis is disrupted when mitochondria generated ROS persists (Liao et al. 2013; Sridharan et al. 2015).

Numerous biological responses occur upon exposure to radiation. Included in these responses are: triggering of signal transduction pathways, gene transcription activation, DNA repair, oxidative stress, inflammation, and cell-cycle arrest.

Collectively, these biological responses are probable factors that determine the fate of irradiated cells (Morgan et al. 1996). Possible fates of irradiated cells would include: repair of damage and restoration of normal function, cell death (via

apoptosis or necrosis), death of cell daughter(s) despite normal reproduction of the irradiated cell, apoptosis-induced cell proliferation, bystander effects and genomic instability-which can lead to neoplastic transformation (Morgan et al. 1996; National Research Council 2006; Stickel et al. 2014; Todd 2003).

HZE particles produce intense ionization because they travel close to the speed of light and because they can be composed of heavy elements. Therefore, HZE particles that traverse cells can cause clusters of DNA damage (also known as multiply damaged sites or microlesions) within localized regions. This damage could include single-strand DNA breaks, double-strand DNA breaks, damage to bases, and abasic sites (Held 2009). It is thought that there are increased biological effects on cells, i.e. cell death, mutagenesis, and neoplastic transformation, due to the inability of cells with complex damage to repair accurately. Studies such as one performed by Desai et al. (2005) suggest both increased and slower processing of DNA damage by monitoring DNA repair proteins and phosphorylated γ -H2AX (Desai et al. 2005; Held 2009). Asaithamby et al. (2008) have also used γ -H2AX to show that as LET increases so does the ability of the cell to repair (Asaithamby et al. 2008).

Genomic instability is included as one the hallmarks of carcinogenesis and radiation exposure has long been linked to increases in cancer incidences (Hall 1994; Morgan et al. 1996). Cancer risk increases when genes involved in DNA response or tumor suppression are impaired (National Research Council 2006). Genomic instability occurs when errors in either cell division or in the ability to maintain proper gene expression cause accrual of alterations or mutations in the genome. These

alterations include: changes in karyotype, gene mutation, gene amplification, cellular transformation, heterogeneity due to clonal expansion, and delayed reproductive cell death. Although both low- and high-LET have been shown to exert negative biological effects, these negative effects increase as LET increases. This is likely due to the fact that high-LET is densely ionizing and causes much more DNA damage within a smaller area. These complex, densely damaged areas are more difficult to repair and thus likely contributors to genomic instability (Morgan et al. 1996; Ward, 1988).

Effects of radiation on cells alone is informative. However, cells within an organism are components of tissues and their regulation depends on their interactions with both other cells and their microenvironment. Just as ionizing radiation elicits a stress response in individual cells, it also does so at the tissue level. Response by damaged tissue occurs by cellular signals including cytokines, growth factors, and chemokines. These soluble signals act to transmit information between cells via their interaction with receptors. They are involved in regulation of cell proliferation and differentiation, motility, adhesion, and apoptosis. Consequences of IR induced changes in the microenvironment include the “activated” phenotype where proteases, growth factors, and persistent ROS production cause quick and continual remodeling of the extracellular matrix (EMC), chronic inflammation (demonstrated as the presence of activated phagocytes and invasion and margination of neutrophils), and production of cytokines like transforming growth factor- β (Barcellos-Hoff et al. 2005).

1.4.2 EVIDENCE FROM CELL AND TISSUE MODELS

Radiation has been shown to affect cells of the central nervous system, although cells within the brain have differing dose tolerances. Cells that are able to divide, such as neuroglia, respond differently to radiation than neurons which cannot. Gobbel et al., 1998 have shown that x-irradiation causes apoptosis in non-cycling neurons despite apoptosis being thought of as generally, only occurring in proliferating cells (Meikrantz and Schlegel 1995; Gobbel et al. 1998). Sun et al. (2013) have also shown that x-irradiation induces neuronal apoptosis via upregulation of Cdk5 and p25 (Sun et al. 2013). DNA damage is probably responsible for apoptosis seen in these neurons since the nucleus and DNA are more radiosensitive than other cell components. Although the CNS is considered a relatively “radio resistant” tissue in comparison to other tissues based on low-LET radiation studies, high doses of low-LET radiation are responsible for brain damage pathogenesis when oligodendrocytes and endothelial cells of the CNS vasculature are damaged (NCRP, 2006; Cucinotta et al. 2009).

Also, Gobbel et al. (1998) showed that despite no differences in the number of DNA strand breaks between neurons and astrocytes, neurons were less efficient at repairing since rejoining of strand breaks occurred more slowly in comparison to astrocytes. Slow repair could be due, in part, to decreased transcription (Hanawalt et al. 1992; Gobbel et al. 1998). These studies are important since neurodegenerative disorders, like Alzheimer’s Disease, may be linked to DNA damage (Chopp et al. 1996; Gobbel et al. 1998).

Understanding the mechanisms involved in radiation induced CNS risks have been made possible with the recent discovery that neurogenesis still occurs in the adult hippocampus. Results of recent studies suggest neuronal stem cells *are* radiosensitive and low-LET radiation affects their proliferation as well as differentiation (Cucinotta et al. 2009; Mizumatsu et al. 2003; Monje et al. 2002; Tofilon and Fike 2000).

Current evidence demonstrates that HZE nuclei cause neurodegeneration. These studies show a dose-dependent decrease in neuronal progenitor cell number in the hippocampus upon exposure to HZE radiation. Additionally, neuronal progenitor cell loss caused altered neurogenesis and resulted in initiation of the inflammatory response-which can also be seen in aged specimens. This suggests the possibility that HZE radiation may be used in future studies to evaluate aging and its processes (Casadesus et al. 2004; Casadesus et al. 2005; Cucinotta et al. 2009; NCRP, 2006).

Ionizing radiation has been shown to cause demyelination of nerve fibers in the cerebral and cerebellar cortex following treatment with IR (Estable-Puig et al. 1964). Demyelination can lead to deficiencies in axonal conduction as well as atrophy and degeneration of axons (Love 2006; McDonald and Sears 1969; Song et al. 2005). These effects can be seen in patients with demyelinating neurological disorders, like multiple sclerosis (MS). In our study, we find degeneration of neurites in the absence of glial cells.

As previously mentioned, IR can cause oxidative stress and inflammation and both have been documented in nervous tissue. In comparison to other tissues, the brain is more susceptible to reactive oxygen species due to its high metabolic rate and increased demand for oxygen (Suman et al. 2013). Recently, the hippocampus has been discovered to contain multipotent neural precursor cells. While it is known that ROS production increases in neuronal cells after IR exposure, these cells have been shown to be hypersensitive to changes in oxidation state. Both x and proton irradiations cause dose dependent increases of ROS in neural precursor cells. *In vivo* data show localization of oxidative stress to cells of the hippocampus. Though unknown at present, oxidative stress could prevent neurogenesis of multipotential neural precursor cells (Cucinotta et al. 2009; Giedzinski et al. 2005). Rola et al. (2005) report reductions in numbers of neural precursor cells in the hippocampal dentate gyrus in a dose and LET dependent manner.

Neuroinflammation is characteristic of brain injury and involves the activation of microglia, astrocytes, and mediators of inflammation. Long term effects can be seen months later when myeloid cells (precursors of adult blood cells) are recruited to damaged regions (Cucinotta et al. 2009; Rola et al. 2005). Low-LET radiation has been shown to upregulate COX-2 production in microglia and may be the cause of neuroinflammation. COX-2 also causes production of prostaglandin E2 which promotes gliosis (Cucinotta et al. 2009; Hwang et al. 2006; Kyrkanides et al. 2002; Moore et al. 2005).

Chronic neuroinflammation is considered to be partly responsible for the diminished cognitive function seen in Alzheimer's patients (Meraz-Ríos et al. 2013). Accumulation of amyloid beta ($A\beta$) in brain parenchyma, referred to as amyloid plaque, is a major histological indicator of AD and is even used as a diagnostic tool (Karran et al. 2011; Cherry et al. 2012). Cherry et al., 2012 recently showed that AD mouse models exposed to ^{56}Fe particle irradiation (a component of GCR) showed increased $A\beta$ plaque accumulation into dense fibrils within the cortex and hippocampus. Additionally, the study found cognitive impairment post irradiation by observing contextual fear conditioning (used to evaluate hippocampal-dependent memory) and a novel object recognition paradigm (a function that relies on many areas of the brain). This strengthens the concern that cognitive impairment and increased risk for development of AD is a concern for astronauts who will be exposed to GCR.

1.4.3 EVIDENCE FROM ANIMAL BEHAVIOR STUDIES

Though evidence is insufficient at this time, current studies suggest that space radiation can cause behavioral and neurological effects. Behavioral changes associated with exposure to space radiation include: sensorimotor deficits and neurochemical changes (Joseph et al. 1992; Joseph et al. 1993; Joseph and Cutler 1994), changes in conditioned taste aversion (CTA) (Hunt et al. 1989; Rabin et al. 1989; Rabin et al. 1991; Rabin et al. 1994; Rabin et al. 2000), changes in operant conditioning (Rabin et al. 2003), and deficits in spatial learning and memory (Shukitt-Hale et al. 2000; Denisova et al. 2002).

Although evidence collected from animal models suggests behavioral and neurological effects can occur upon exposure to space radiation, behavior is an endpoint that is difficult to evaluate. Because of this, large variations in animal studies monitoring behavior in response to radiation have been reported and are likely due to the different species, strains, and method used to evaluate (NCRP, 2006; Cucinotta et al. 2009). However, in order to understand behavioral changes, we need to understand what changes are occurring at the cellular level in the CNS.

Immediate CNS effects are also a concern and include anorexia and nausea. Rabin et al. performed a study to evaluate how varying forms of radiation causes vomiting in ferrets. (Rabin et al. 1994). These prodromal effects serve to help estimate exposure dose since they are dose-dependent. Development of degenerative diseases may be due to increases in cytokines and chemokines that are correlated with these acute CNS effects (Cucinotta et al. 2009).

1.4.4 EVIDENCE FROM HUMAN DATA

Current evidence documenting the effects of ionizing radiation comes from patients receiving radiotherapy for cancer treatment. Effects of radiation therapy can provide insight into possible CNS risks to astronauts, despite being a form of terrestrial radiation and higher doses than will be experienced beyond LEO.

Lower doses of radiotherapy have been shown to cause neurocognitive effects, with children being more sensitive (Schultheiss et al. 1995; BEIR-V, 1990). Children who

have undergone radiation treatment for brain tumors have experienced decreases in academic achievement and intelligence (as shown in IQ tests) as well as deficits in cognitive control (management of cognitive processes) (Butler and Haser, 2006). Additionally, fetuses exposed to radiation between 8-15 weeks post-conception during atomic bombing in Japan expressed mental retardation (BEIR-V, 1990). It should be noted that developing brains are far more sensitive than fully developed brains to damaging agents.

Deficits in cognitive functioning, language acquisition, visual spatial ability, memory, executive functioning, and differences in social behavior (chronic fatigue and depression) (Tofilon and Fike, 2000) have all been seen in patients whose tumors were treated with charged particle beams. Although chemotherapy is often used in conjunction with radiotherapy, none of these deficits were seen with chemotherapy alone and therefore can be attributed to either radiation alone or to a combination of chemotherapy and radiation (Cucinotta et al. 2009).

Using astronauts involved in past NASA space missions is unlikely to reveal any CNS effects caused by radiation. This is because the population of astronauts is incredibly low. Also, previous missions were of short duration and astronauts did not travel beyond LEO and were therefore protected by Earth's magnetic field. Thus far, risk prediction of radiation exposure comes from data collected from survivors of atomic bomb events. However, this is terrestrial radiation and is not

representative of radiation from GCR and SPEs that would be encountered in space (Cucinotta et al. 2001).

1.4.5 COMBATING EFFECTS OF RADIATION

Before manned space missions into deep space can occur, it is imperative that we fully assess the risks associated with such missions. Understanding the risks and effects of galactic cosmic radiation and HZE particles on the central nervous system will allow for the development of countermeasures that would combat the adverse effects of space radiation. Such studies are already underway. Based on animal studies, use of antioxidants and anti-inflammatory agents are probable biological countermeasures (Rabin et al. 2005). Another likely countermeasure would include targeting and eliminating (via apoptosis) cells damaged by GCR (Cucinotta et al. 2009) thus decreasing the chances of genomic instability.

1.5 RADIATION THERAPY

Approximately 20% of our radiation exposure is due to man-made radiation; nearly all of it (about 96%) is due to medical procedures (U.S. Nuclear Regulatory Committee). In 2006, about 435 million medical procedures involving ionizing radiation were performed in United States (NCRP, 2009). Currently, only 47 active astronauts are employed by NASA; and it is likely not all of them will have a mission to space. So perhaps more relevant are the effects on the CNS of patients undergoing radiation therapy for cancer treatment or for medical procedures like CT scans.

According to the Central Brain Tumor Registry of the United States (CBTRUS), nearly 700,000 Americans were living with either primary brain or CNS tumors in 2010. CBTRUS estimates 77,670 new cases of CNS tumors for 2016, about 32% of those being malignant (CBTRUS, 2014).

Radiation, along with chemotherapy, is widely used to treat primary and metastatic brain tumors. Despite advances in radiation therapy its usage is restricted to limit exposure to healthy tissue. Radiation therapy itself can cause neurological and CNS toxicity making it difficult to recognize radiation induced damage from the effects of the cancer alone.

Complications of radiation are categorized into acute (during or immediately following), early delayed (weeks to months), and late delayed (months to years) (Goldberg et al. 1982; Rinne et al. 2012). Acute encephalopathy occurs within hours or days of radiation therapy and typically in patients that undergo large daily dose fractions. Symptoms include headaches, nausea, lethargy, vomiting, seizures, and fever. Early delayed complications occur within two to three months of exposure and is thought to be due to demyelination. Symptoms are not dissimilar to acute complications and include headache, lethargy, nausea, irritability, and swelling of the optic disc(s). Unlike acute and early delayed complications, late delayed radiation effects are often irreversible and continue to progress. Included in the late delayed radiation induced CNS effects are radio necrosis and leukoencephalopathy. Radio necrosis develops when there is damage to white matter of the brain or the

spinal cord causing necrosis, vascular injury, and damage and death to both axons and oligodendrocytes. Leukoencephalopathy (loss of white matter) results in cognitive dysfunction such as short-term memory loss and impairments in judgement, attention, and executive functioning. Additionally, irradiation of the cranium for cancer treatment causes a 7-fold increase in developing secondary brain tumors. Secondary brain malignancies associated with CNS irradiation include meningiomas, gliomas, and sarcomas (Rinne et al. 2012).

1.6 OUR FOCUS

Neuronal function is dependent on proper structure and synaptogenesis. Any disruption in neurite architecture, like retraction of neurites, defects in cytoskeleton dynamics, and neuronal cell death could cause diminished neuronal function. Additionally, the critical function of glial cells in maintaining neuronal function and their implication in degenerative diseases force the need to study their response to radiation. If space radiation has potential to cause damage to neurites and glial cells- and therefore function of the CNS, resources need to be allotted to reducing harm to astronauts as they travel outside of Earth's protective magnetic field.

This study uses the SH-SY5Y, C6, and CL-mPG-15 cell lines to examine effects of radiation. SH-SY5Y is a neuroblastoma cell line sub cloned from the SK-N-SH line. The SK-N-SH line was established in 1970 from the bone marrow biopsy of a four-year-old female (Biedler et al. 1973). Neuroblastomas are tumors that affect small children, usually under the age of 10, and are derived from immature nerve cells of

the sympathetic nervous system (SNS) ([Edsjö et al. 2007](#)). SH-SY5Y cells have widely been used as an *in vitro* model for neurotoxicity experiments ([Cheung et al. 2009](#)), neuronal differentiation ([Edsjö et al. 2007](#)) and outgrowth ([Dwane et al. 2013](#)), as well as Parkinson's disease and Alzheimer's disease studies ([Constantinescu et al. 2007](#); [Dwane et al. 2013](#)).

C6 is a glioma cell line. It was derived from chemically inducing glial brain tumors in random-bred Wistar-Furth rats using N,N'-nitroso-methylurea ([Amberger et al. 1998](#); [Grobben et al. 2002](#)). These tumors are morphologically similar to glioblastoma multiforme (GBM), an aggressive type of glioma that is resistant to traditional therapeutic methods, including radiation ([Grobben et al. 2002](#)). The CL-mPG-15 is a primary glial cell line established from the brains of mice aged postnatal days 1-5. Primary cells are more representative of those found *in vivo* and are not tumorigenic.

Although space exploration is fascinating and important, more relevant is the likely damage to substantial numbers of patients exposed to radiation for cancer treatment. Radiation can rid or halt growth of cancer cells but care needs to be taken to study the long-term effects of radiation treatment as well as to mitigate its potential damage.

2: MATERIALS AND METHODS

2.1 CELL CULTURE

2.1.1 SH-SY5Y Cell Line

SH-SY5Y cells were purchased from the American Type Culture Collection (ATCC, Manassas, VA,) and maintained in a 1:1 mixture of EMEM and F12K media supplemented with 10% fetal bovine serum (ATCC), 100 µg/mL streptomycin, and 100 U/mL penicillin (Lonza, Walkersville, MD). Cells were cultured in T-25 plug seal tissue culture flasks (Corning, Corning, NY) and incubated at 37 °C and 5% CO₂ in a Forma™ Series II 3110 Water-Jacketed incubator (ThermoScientific, Marietta, OH). Subculturing was done by removing medium from the flasks then rinsing cells with Ca²⁺/Mg²⁺ free Dulbecco's phosphate-buffered saline (DPBS) (Mediatech, Inc., Manassas, VA), and detaching using 0.25% trypsin/2.21 mM EDTA (Corning). Trypsin was quenched with the equal volume of medium. Cells were counted using a hemocytometer (Hausser Scientific, Horsham, PA) with 0.2% trypan blue (Lonza). Passaging occurred weekly and medium was refreshed every 4-7 days.

For all experiments, SH-SY5Y cells were differentiated with 10 µM all-trans retinoic acid (Sigma, St. Louis, MS), allowed to differentiate for 5 days to ensure adequate neurite outgrowth, then treated with the desired dose of x-ray radiation unless otherwise noted.

2.1.2 C6 Cell Line

C6 cells were purchased from the American Type Culture Collection (ATCC, Manassas, VA,) and maintained in F-12K medium supplemented with 2.5% Fetal Bovine Serum (FBS), 15% Horse Serum (ATCC), and 100 µg/mL streptomycin/100 U/mL penicillin (Lonza). Cells were cultured in T-25 plug seal tissue culture flasks (Corning) and incubated at 37 °C and 5% CO₂ in a Forma™ Series II 3110 Water-Jacketed incubator (ThermoScientific). Subculturing was done by removing medium from the flasks, rinsing cells with Ca²⁺/Mg²⁺ free Dulbecco's phosphate-buffered saline (DPBS), and detached using 0.25% trypsin/2.21 mM EDTA (Corning). Trypsin was quenched with the equal volume of medium. Cells were counted using a hemocytometer (Hausser Scientific) with 0.2% trypan blue (Lonza). Passaging occurred every three days, medium did not need to be refreshed. For all experiments, C6 cells were allowed to rest and enter normal cell cycle for 72 hours before being treated with the desired dose of x-ray radiation unless otherwise noted.

2.1.3 CL-mPG-15 Cell Line

CL-mPG-15 cell line was established from the brains of mice aged postnatal days 1-5; brains were graciously donated by Dr. Leif Oxburgh of Maine Medical Center Research Institute (MMCRI). Upon sacrifice and dissection, brains were kept in HIBERNATE in order to preserve viable brain tissue. Brain tissue was then digested with 2.5% Trypsin EDTA (Corning) and plated into 12 well plates. Media was refreshed after 24 hours and again every 48 hours until confluent at which cells

were subcultured and transferred to culture flasks. Cells were maintained in Dulbecco's Modified Eagle's Medium (DMEM, Lonza) supplemented with 10% FBS, 100 µg/mL streptomycin/100 U/mL penicillin (Lonza), and 1% Glutamax (Gibco, Life Technologies, Grand Island, New York). Cells were cultured in T-25 plug seal tissue culture flasks (Corning) and incubated at 37 °C and 5% CO₂ in a Forma™ Series II 3110 Water-Jacketed incubator (ThermoScientific). Subculturing was done by removing medium from the flasks, rinsing cells with Ca²⁺/Mg²⁺ free Dulbecco's phosphate-buffered saline (DPBS), and detached using 0.25% trypsin/2.21 mM EDTA (Corning). Trypsin was quenched with the equal volume of medium. Cells were counted using a hemocytometer (Hausser Scientific) with 0.2% trypan blue (Lonza). Passaging occurred once a week and medium was refreshed every 4 days. For all experiments, CL-mPG-15 cells were allowed to rest and enter normal cell cycle for 72 hours before being treated with the desired dose of x-ray radiation unless otherwise noted.

2.2 PRELIMINARY EXPERIMENTS

Preliminary testing was done to determine appropriate seeding densities for each cell line and assay performed. For phase contrast microscopy and immunocytochemistry assays with the 5Y cell line, various densities were seeded, treated with retinoic acid, and allowed to grow for 5 days before a visual inspection of each density was done to ensure neither scarce nor crowded cell growth. Seeding densities and incubation times for MTS assay were done by creating a metabolic

curve for each cell line. Absorbance readings were taken for incubation hours at 1, 2, 3, and 4 hours for each seeding density.

Preliminary dose testing was done in order to establish which radiation doses would yield cytotoxic effects and be used in all subsequent experiments. SH-SY5Y cells were the basis for all experiments and all subsequent cell lines tested used the same radiation doses as the 5Y cell line.

2.3 TREATMENT

Cells were treated using a Faxitron x-ray system. Cells are placed into the x-ray cabinet and treated accordingly, depending on dose desired. Radiation exposure is dependent on the distance from the tube (shelf height) and energy settings (kVp). Doses range from 0 to 20 Gy for all cell lines, although preliminary doses up to 200 Gy were performed.

NOTE: Although this project is aimed to look at the effects of radiation that would typically be encountered in space, there are two arguments to why we are using x-ray radiation instead. Particle accelerators, like the one at CERN, have limited time allotted for independent labs like ours and you are only granted time if you have a substantial grant and are well known. The University of Southern Maine has a Faxitron x-ray cabinet capable of treating with x-rays and therefore it is more efficient and less costly than treating with particles. Additionally, there are only a

few astronauts that will be exposed to GCR; whereas there are far more people exposed to x-ray radiation from medical procedures or from radiation therapy.

2.4 PHASE CONTRAST MICROSCOPY

Phase contrast microscopy was used to analyze neurite length which indirectly monitors neurite retraction in SH-SY5Y cells. Phase contrast is a technique used to examine unstained specimens where structures are similar in transparency. By exploiting differences in refractive indexes, structures can be viewed and identified.

A double t (‡) was scratched onto the bottom of four wells of a 24 well plate (VWR, Batavia, IL) using a diamond knife to ensure the observation of the same field of view and cells over time. SH-SY5Y cells were seeded at 1,750 cells/well, six wells were seeded for each dose, and cells were allowed to differentiate for 5 days before being treated. A random quadrant of the double t was chosen and recorded. Images of both the scratch and cells allows for analysis of the same area of the plate and presumably, the same cells over time. Images were taken immediately prior to treatment and again after 6, 24, and 48 hours post treatment using a TS100 phase-contrast microscope (Tokyo, Japan) at 200X magnification, a Diagnostic Instruments SPOT RT Color camera (Sterling Heights, MI), and SPOT Advanced 4.0.9 software. Before analysis, images were coded to ensure no bias by treatment dose or time post-treatment. Analysis was done using ImageJ software; where neurite length, cell number, and neurite complexity (number of branch points) were quantified. Data were imported to GraphPad Prism 7 to be analyzed and graphed. Data represent at

least three independent experiments analyzed with a two-way ANOVA with Dunnett's multiple comparisons post-test where $p \leq 0.05$ denotes statistical significance.

2.5 IMMUNOCYTOCHEMISTRY

2.5.1 Cytoskeleton Staining of SH-SY5Y Cells

Immunocytochemistry is a method used to detect proteins or other macromolecules by use of primary antibodies that bind them. Secondary antibodies conjugated with fluorophores allows for visualization of the target by using a fluorescence microscope. Immunocytochemistry was used to monitor the cytoskeleton components, actin and microtubules, to monitor changes in neurites and growth cones exposed to irradiation over time. Neurite retraction was examined as well as number of collapsed growth cones. Growth cones were considered collapsed if no actin was observed in the tip of the neurite or growth cone.

Mouse anti- α -tubulin was used as the primary antibody to bind microtubules; AlexaFluor 555 goat-anti-mouse was used as the secondary. Filamentous actin (F-actin) was stained using AlexaFluor Phalloidin 488, which is fluorescently labeled phalloidin. Phalloidin is a toxin isolated from *Amanita phalloides*, or death cap mushroom and prevents the depolymerization of F-actin.

SH-SY5Y cells were seeded into 4-well chamber slides (Nunc Lab-Tek, Rochester, NY) at 1,750 cells/well then allowed to rest for 5 days in order to grow sufficient

neurites. Since two time points were used, two identical slides were seeded to in order to observe cytoskeleton structure 0 and 24 hours post-irradiation. Cells were then treated with X-irradiation (either 0, 5, or 10 Gy). Slides marked 0 hour were fixed immediately after treatment and stored in PBS while those marked 24 hour were put into the incubator and fixed the following day. This allows remaining immunocytochemistry steps to be done concurrent with both time points.

After treatment and incubation, cells were fixed with PHEM buffer (60 mM PIPES, 25 mM HEPES, 10 mM EGTA, and 2 mM MgCl₂), 4% paraformaldehyde, 0.5% glutaraldehyde, and 1% Triton-X 100. To fix, 250 uL of media was removed from each well and replaced with 250 uL of fix and allowed to incubate at room temperature for 7 minutes. 250 uL of medium/fix was again removed and replaced with fix and incubated at room temperature for 7 minutes. After this second incubation, all medium was removed and replaced with 500 uL of fix and incubated at room temperature for 7 minutes. Neurites are delicate and slow removal and addition of medium/fix allows a more gentle fix ensuring neurites are not damaged by disturbance from adding more liquid to the wells. However, once fixation is complete neurites are bound to the slide more firmly and able to withstand more turbulence from future staining steps. Cells were washed and permeabilized with PBS and 0.3% Triton-X 100 (PBS-TX) for 30 minutes then blocked with 10% goat serum in PBS-TX for 30 minutes at room temperature. Liquid was removed from each well and 350 uL of unconjugated mouse anti- α -tubulin (1:200) (Thermo Fisher Scientific, Waltham, MA) was added and left to incubate for 1 hour at room

temperature. Cells were washed with PBS-TX twice for 5 minutes. Next, 350 μ L of Alexa 555 (1:500) (Thermo Fisher Scientific, Waltham, MA) in PBS-TX was added to each well and allowed to incubate for 1 hour at room temperature in a drawer to prevent bleaching of the fluorescent stain. Laboratory lights were also off or dim from this step forward. Cells were thrice washed with PBS for 5 minutes; PBS-TX cannot be used for future steps as it interferes with phalloidin. Next, 350 μ L of Alexa 488 Phalloidin (1:100) (Thermo Fisher Scientific, Waltham, MA) in PBS was administered to each well and allowed to incubate at room temperature for 2 hours. Cells were then washed with PBS twice for 5 minutes and the slide chamber gaskets and seals were removed. Before PBS could dry one drop of Prolong Gold antifade reagent with DAPI (Thermo Fisher Scientific, Waltham, MA) was added to each well and coverslips were applied. Slides were allowed to cure at room temperature underneath a dark box or in a lab drawer and subsequently stored at 4°C until analysis.

For epifluorescent microscopy, an Olympus IX71 microscope equipped with an Olympus U-CMAD3 camera was used to photograph images. Nikon NIS-Elements software was used to acquire images. Analysis was done using ImageJ software; where neurite length and number of collapsed growth cones per 100 cells were quantified. Data were imported to GraphPad Prism 7 to be analyzed and graphed. Data represent at least three independent experiments analyzed with a two-way ANOVA with Dunnett's multiple comparisons post-test where $p \leq 0.05$ denotes statistical significance.

2.5.2 GFAP Staining of Primary Glial Cell Line

Glial fibrillary acidic protein (GFAP) staining was used to confirm the CL-mPG-15 cell line was glial in origin. GFAP is an intermediate filament protein that is used to support and strengthen cells. GFAP comprises a portion of the cytoskeleton of astrocytes and immunostaining for GFAP has been used to identify and glial cells from other cell populations.

CL-mPG-15 cells were fixed with PHEM buffer (60 mM PIPES, 25 mM HEPES, 10 mM EGTA, and 2 mM MgCl₂), 4% paraformaldehyde, 0.5% glutaraldehyde, and 1% Triton-X 100. Cells were washed and permeabilized with PBS and 0.3% Triton-X 100 (PBS-TX) for 30 minutes then blocked with 10% goat serum in PBS-TX for 30 minutes at room temperature. Cells were rinsed with PBS followed by a 60-minute room temperature incubation with Polyclonal Rabbit Anti-Glial Fibrillary Acidic Protein (1:500) (Dako, Carpinteria, CA). Cells were then washed with PBS twice for 5 minutes and the slide was allowed to dry in a dark box. For epifluorescent microscopy, an Olympus IX71 microscope equipped with an Olympus U-CMAD3 camera was used to photograph images. Nikon NIS-Elements software was used to acquire images.

2.6 MTS ASSAY

The MTS assay is a colorimetric method that and allows for analysis of cell number or cytotoxicity. MTS (3-(4,5-dimethylthiazol-2-yl)-5-(3-carboxymethoxyphenyl)-2-(4-sulfophenyl)-2H-tetrazolium) is a tetrazolium salt that is bio reduced to a colored

formazan product by mitochondrial dehydrogenase enzymes within viable cells.

Formazan absorbs best at 490 nm. Promega's (Madison, WI) CellTiter 96® AQueous One Solution Cell Proliferation Assay was used to monitor cellular metabolic activity and therefore viability in both irradiated and nonirradiated cells.

For all cells lines, cells were plated into 96-well clear bottom tissue culture treated plates (BD Falcon, San Jose, CA). Before experiments began, metabolic curves using MTS were performed to determine appropriate seeding densities and incubation times for each cell line. Briefly, various densities were seeded into wells of a 96 well plate. Since incubation in MTS reagent varies with each cell line absorbance readings were taken at 1, 2, 3, and 4 hours for each cell line.

SH-SY5Y cells were seeded at 50,000 cells/well and differentiated as noted above and allowed to rest for 120 hours. Both C6 and CL-mPG-15 cell lines were seeded 5,000 cells/well and allowed to rest for 48 hours. Cells were then treated with 0, 1, 5, 10, or 20 Gy of irradiation. Plates were read at 0, 24, and 48 hours post-treatment in order to monitor cell viability after treatment over time. Once treated, 20 uL of MTS solution was added to each well and allowed to incubate for either 3 (C6) or 4 hours (SH-SY5Y and CL-mPG-15 cell lines) in order for the product to form. It should be noted that all three time points were plated on the same plate, however, MTS was only added to the time point of interest. Additionally, since the MTS assay requires incubation, the 0 hour time point is actually 3 or 4 hours depending on cell line.

A BioTek Synergy HT plate reader (BioTek Instruments, Inc., Winooski, VT) was used to measure absorbance of formazan at 490 nm. Because plates needed to stay sterile, they were read with lids on. Due to multiple plates being read at the same time, the opening and closing of the incubator caused condensation on the lids of all plates. Because condensation can potentially alter absorbance readings, it was imperative to minimize its presence. Although the plate reader was prepared to be at 37 °C, the same temperature as the incubator, condensation persisted. Placing all plates into the tissue culture hood with lids off for 1 minute helped reduce or eliminate condensation. Data were imported to GraphPad Prism 7 to be analyzed and graphed. Data represent at least three independent experiments analyzed with a two-way ANOVA with Dunnett's multiple comparisons post-test where $p \leq 0.05$ denotes statistical significance.

3: RESULTS

3.1 Preliminary Experiments (seeding density and dose testing)

Before experiments that aimed to answer our hypotheses were performed it was important to preliminary experiments to find appropriate seeding densities and radiation doses. Seeding density is essential as it ensures enough cells are present to analyze but not too dense to inhibit visualization of independent neurites (for phase contrast microscopy) or promote contact inhibition of cell division (MTS assay).

Phase contrast microscopy and immunocytochemistry experiments were used to analyze neurite morphology and cytoskeleton structure and therefore only SH-SY5Y cells were examined. Visual inspection of preliminary seeding density experiments for the SH-SY5Y cell line showed that seeding at 1,750 cells per well is appropriate for phase contrast microscopy and immunocytochemistry experiments (Figure 1). All other seeding densities are either too scarce or too dense and would not allow accurate results.

Seeding densities for MTS assay were chosen by creating a metabolic curve for each cell line where absorbance was measured for each density over four incubation periods. Seeding densities examined for the SH-SY5Y cell line were 10×10^3 , 20×10^3 , 30×10^3 , 40×10^3 , 50×10^3 , 60×10^3 , 70×10^3 , 80×10^3 , 90×10^3 , and 10×10^4 cells/well. Absorbance ranges from 0.01 to 0.40 for 1 hour incubation, 0.20 to 0.70 for 2-hour incubation, 0.29 to 0.97 for 3-hour incubation, and 0.31 to 1.26 for 4-hour incubation (Figure 2). Absorbance increases until plateauing around 70,000 cells/well for all incubation periods. Based on these data, 50×10^3 cells/well was the chosen seeding density. Four-hour incubation resulted in the highest absorbance readings for all cell densities and was therefore used in MTS experiments.

Seeding densities examined for the C6 cell line included 1×10^3 , 2×10^3 , 3×10^3 , 4×10^3 , 5×10^3 , and 6×10^3 cells/well. Absorbance ranges from 0.68 to .49 for 1 hour incubation, 1.20 to 1.07 for 2-hour incubation, 1.41 to 1.03 for 3-hour incubation, and 1.59 to 1.02 for 4-hour incubation (Figure 3). Based on these data, 5×10^3

cells/well was the chosen seeding density. A 3-hour incubation was chosen since there wasn't a significant difference between 3 and 4-hour incubation times.

Seeding densities examined for the m-15 cell line included 2×10^3 , 3×10^3 , 4×10^3 , and 5×10^3 cells/well. Absorbance ranges from 0.014 to 0.082 for 1 hour incubation, 0.88 to 0.19 for 2-hour incubation, 0.13 to 0.26 for 3-hour incubation, and 0.17 to 0.31 for 4-hour incubation (Figure 4). Based on these data, 5×10^3 cells/well was the chosen seeding density. Because absorbance readings were so low a 4-hour incubation time was chosen. Seeding densities for all cell lines and assays can be seen in Table 1.

Radiation dose testing was dependent on the SH-SY5Y cell line for all assays. For phase contrast microscopy and immunocytochemistry assays, doses were chosen so that apparent cell death was present but not absolute. Visual inspection lead to doses of 0, 0.05, 1, 5, and 10 Gy for phase contrast microscopy and immunocytochemistry experiments (data not shown). Radiation doses over 10 Gy resulted in substantial cell death, particularly 24 hours post-treatment, whereas minimal numbers of cells were left and sample size would not yield accurate results.

Dose testing for MTS assay was performed, and based on metabolic activity of the SH-SY5Y cell line, doses of 0, 1, 5, 10, and 20 Gy were chosen (Figure 5). The highest dose, 20 Gy, was chosen because it caused considerably lower absorbance readings in comparison to control cells, 0.66 and 1.06 respectively. Doses between control and 20 Gy were objectively chosen so that dose increments made sense. These doses

were used for all cells lines; however, additional dose testing was done on both C6 and CL-mPG-15 cell lines (Figures 6 and 7, respectively). C6 glial cells treated with 500 Gy, a markedly huge dose of radiation, had absorbance readings higher than control cells 48 hours post-treatment (1.47 and 0.73, respectively) (Figure 6). Primary glial cells of the m-15 cell line had lower base absorbance readings. Yet, cells exposed to 200 Gy at 48 hours post-treatment still had absorbance readings not dissimilar to control cells, 0.32 and 0.39, respectively (Figure 7).

Preliminary experiments were also needed to confirm that the primary glial cell line, CL-mPG-15, expressed glial fibrillary acidic protein (GFAP). Preliminary immunocytochemistry experiments show cells of the CL-mPG-15 cell line fluoresce when exposed to anti-GFAP antibodies and examined with a fluorescence microscope (Figure 8).

3.2 Effects of Radiation on Differentiated SH-SY5Y Morphology

Phase contrast microscopy was used to observe the effects of radiation on SH-SY5Y morphology. Neurite retraction was investigated by measuring neurite length while counting number of branch points, which enabled examination of neurite complexity. Additionally, cell number was analyzed in order to monitor cytotoxicity (in addition to MTS assay).

Counting viable cells using phase contrast microscopy was supplementary as the MTS assay was used to examine the cytotoxicity of radiation in all cell lines.

However, considering images were already collected and the ease of analyzing using ImageJ, phase contrast microscopy enabled us to compare cytotoxicity findings of two different assays within the SH-SY5Y cell line. Using a two-way ANOVA and Dunnett's multiple comparisons post hoc test, none of the doses immediately following treatment (0 hour) significantly differed in cell number to controls (Figure 9). Cell number significantly decreased from 38.8 (control) to 35.6 six hours post-treatment between control cells and cells treated with 5 Gy ($p < 0.01$). All radiation doses at both 24 and 48 hours post-treatment had significantly reduced cell numbers in comparison to controls.

Effects of radiation on neurite retraction was assessed by averaging the longest neurite per soma in each dose and time group. Phase contrast microscopy suggests neurite length does not change with either dose or time (Figure 10). Using a two-way ANOVA and Dunnett's multiple comparisons post hoc test, there were no significant differences in neurite length between non-irradiated and irradiated cells at any time point.

Determining radiation's effect on neurite complexity was based on counting the number of branch points per neurite. Number of branch points decreased in differentiated SH-SY5Y cells in select dose and time groups (Figure 11). Cells treated with 1 Gy had decreased number of branch points in comparison to controls at 6 and 24 hours post-treatment ($p < 0.05$). A radiation dose of 5 Gy at 48 hours post-treatment also had significantly reduced branching when compared to control cells

($p < 0.001$). All other doses and time points were not significantly different than control cells.

3.3 Effects of Radiation on SH-SY5Y Cytoskeleton Structure

Immunocytochemistry was used in order to monitor changes of SH-SY5Y cytoskeleton structure in response to radiation. Neurite length and number of collapsed growth cones were examined. Prior to conducting experiments, immunocytochemistry staining was tested in order to confirm the protocol and ensure dyes were working (Figure 12). DAPI stained DNA/nuclei. Anti-tubulin coupled with an AlexaFluor555 secondary stained microtubules. AlexaFluor Phalloidin 488 stained actin. Merged images depict all dyes stacked.

Neurite length was also analyzed using immunocytochemistry. This enabled data comparisons between the two assays. Just as in phase contrast microscopy, effects of radiation on neurite retraction was assessed by averaging the longest neurite per soma in each dose and time group. Neurite length of differentiated SH-SY5Y cells decreases with radiation dose and time based on immunocytochemistry (Figure 13). Neurites of non-irradiated cells averaged 59.1 and 62.8 μm at 0 and 24 hours, respectively. Treated cells had significantly shorter neurites at both time points. Neurites of cells exposed to 5 Gy averaged 48.3 and 47.0 μm at 0 and 24 hours, respectively while those exposed to 10 Gy averaged 42.9 and 38.8 μm at 0 and 24 hours, respectively.

Visual analysis of cytoskeleton components is valuable and should not be underestimated. Immunocytochemistry allows for such visual data to be collected and presented alongside data displayed in graphs or tables. Control cells 48 hours post-treatment tend to exhibit complicated cytoskeleton structure (Figure 14). Microtubules along the neurite shaft are elongated and bundled while actin networking and branching is complex. Irradiated SH-SY5Y cells possess the same overall cytoskeleton organization seen in control cells, although they tend to be shortened and less complex (Figure 15). However, morphologies vary significantly in both treated and untreated populations and therefore it is possible to see less complex cells in control cultures (Figure 16) and long neurites in irradiated cultures (Figure 17).

Immunocytochemistry allowed visualization of the growth cone and its structure which ultimately, enabled monitoring of growth cone collapse. The number of collapsed growth cones does not change with dose or time (post-treatment) between SH-SY5Y control cells and x-ray treated cells (Figure 18). Means for 0, 5, and 10 Gy treatments at 0 hour were 2.000, 2.463, and 3.307, respectively. Means for 0, 5, and 10 Gy treatments 24 hours post-irradiation were 2.227, 3.558, and 4.296, respectively. Though not significant, data do show a trend where number of collapsed growth cones is higher as dose increases. Additionally, all 24-hour post-treatment time points were higher than 0-hour time-points for all treatments.

3.4 Cytotoxicity of Radiation

Cytotoxicity of x-ray radiation was monitored using the MTS assay. Changes in absorbance at 490 nm are correlated with cell viability e.g. higher absorbance readings are associated with higher rates of metabolic activity while lower readings are associated with decreased metabolic activity.

3.4.1 MTS Assay of SH-SY5Y Cell Line

X-ray radiation causes a decrease in metabolic activity in SH-SY5Y cell line (Figure 19). All treatments had approximately the same absorbance readings 4 hours post exposure at around 0.625. At 24 hours post treatment absorbance values decreased as dose increased; cells exposed to 1 Gy irradiation did not significantly differ from control cells at this time point. Exposures of 5, 10, and 20 Gy had absorbance readings of 0.530, 0.472, and 0.403, respectively, and significantly differed from control cells which had an absorbance reading of 0.622. Post-treatment time of 48 hours showed a difference only between control cells and those treated with 10 and 20 Gy ($p < 0.05$, $p < 0.001$, respectively).

3.4.2 MTS Assay of C6 Cell Line

X-ray radiation causes an initial increase and subsequent decrease in metabolic activity in the C6 glial cell line as determined by the MTS assay (Figure 20). Absorbance readings at 24 hours were higher than those at 3 hours, however at each of these time points values for all treatments were similar. Absorbance

readings 48 hours post-treatment were highest with cells exposed to 20 Gy (0.164) and decreased with dose, control cells having the lowest absorbance (0.838). This trend, despite being counter-intuitive, was evident in all trials. Cells treated with 1 Gy did not differ in absorbance from control cells 48 hours post exposure while those treated with 5, 10, and 20 Gy did ($p < 0.001$, $p < 0.0001$, and $p < 0.0001$, respectively).

3.4.3 MTS Assay of CL-mPG-15 Cell Line

X-ray radiation causes a decrease in metabolic activity over time in the m-15 cell line as determined by the MTS assay (Figure 21). Absorbance values did not differ between treatments at 4-hour time point. Absorbance readings increased for all treatments from 0 to 24 hours post exposure. All doses, 1, 5, 10, and 20 Gy significantly differed from control cells with $p < 0.01$, $p < 0.0001$, $p < 0.0001$, $p < 0.0001$, respectively. Absorbance readings increased for control and 1 Gy exposed cells from 24 to 48 hours, while all other doses decreased. All treatment groups significantly differed from the control where $p < 0.0001$.

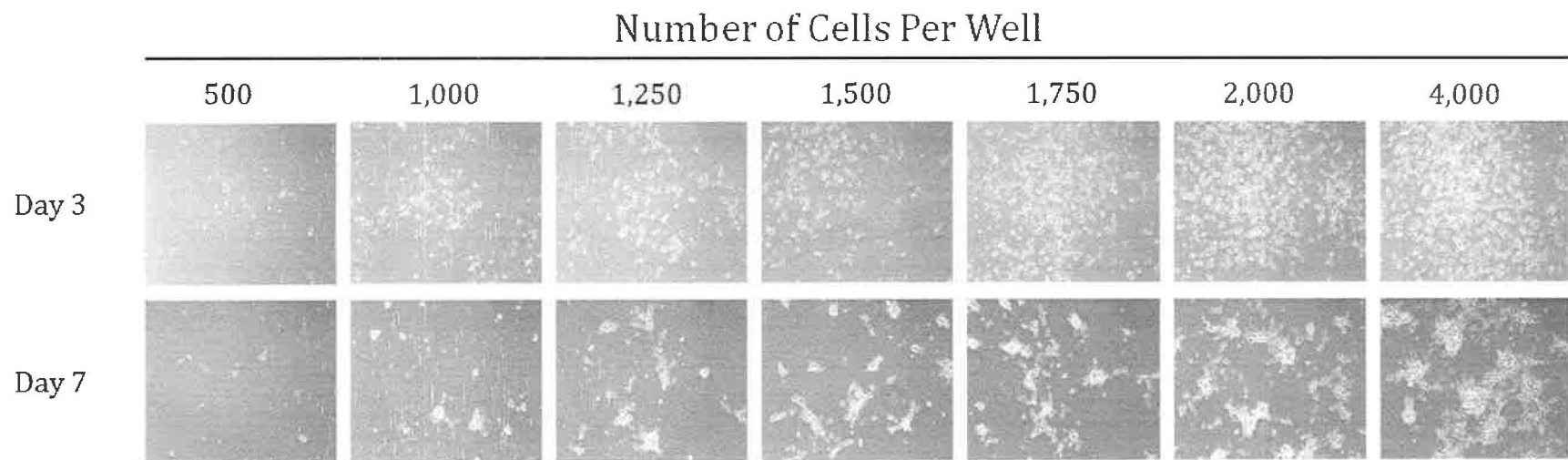


Figure 1: Images used to determine appropriate seeding density of SH-SY5Y cell line for phase contrast microscopy and immunocytochemistry assays.

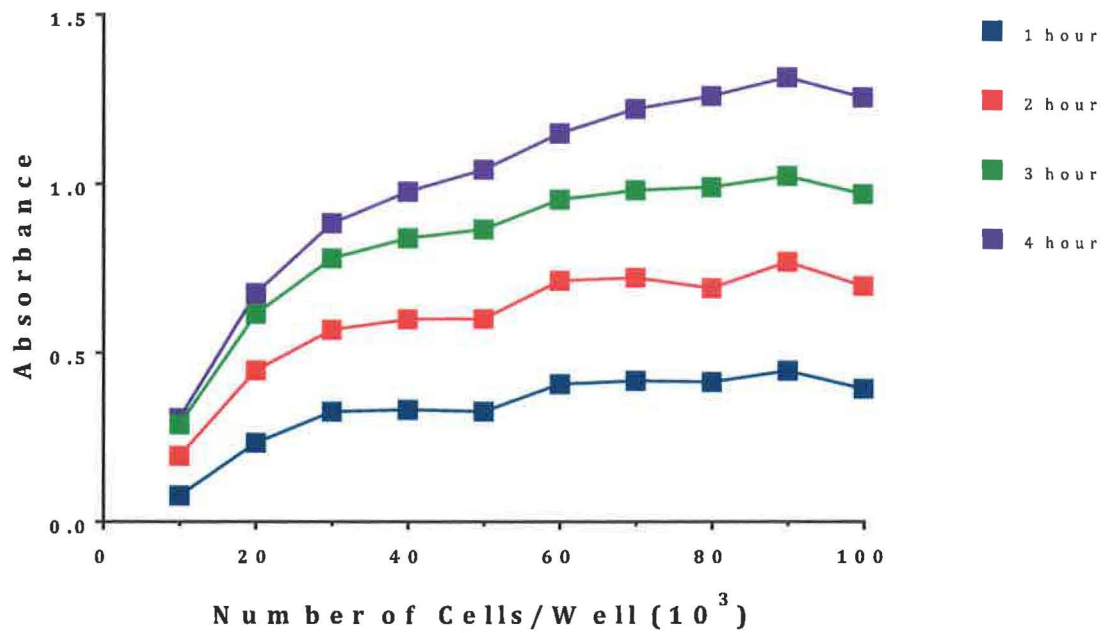


Figure 2: Metabolic curve for SH-SY5Y cell line. Preliminary MTS assay performed to determine appropriate seeding density and MTS incubation period for SH-SY5Y cell line. Based on results a seeding density of 50,000 cells/well was chosen with a 4 hour MTS incubation for subsequent MTS assays regarding the SH-SY5Y cell line.

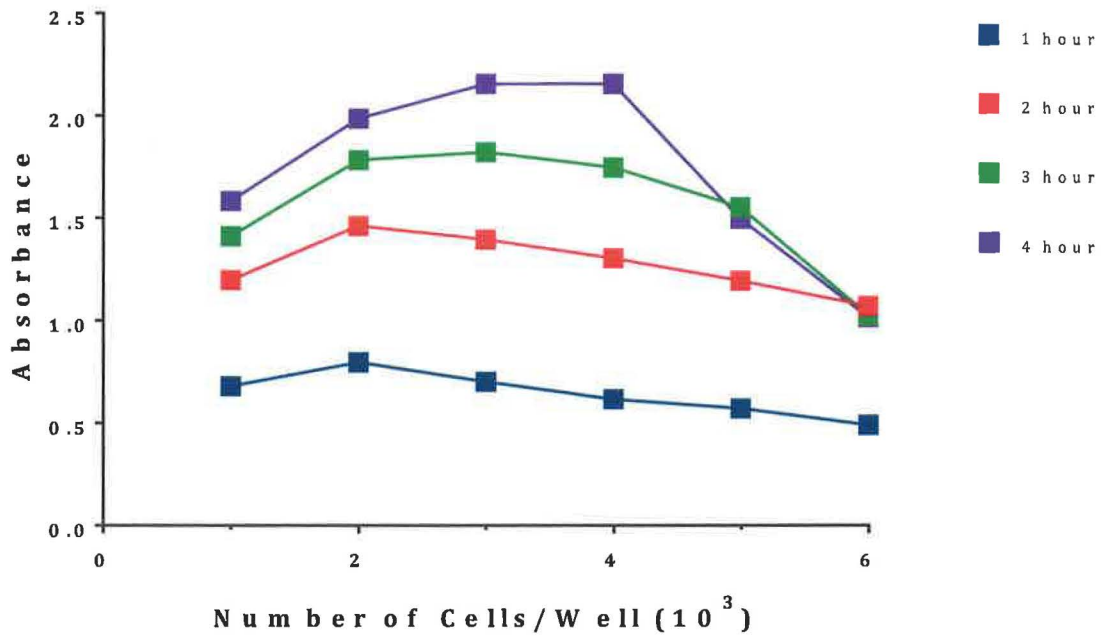


Figure 3: Metabolic curve for C6 cell line. Preliminary MTS assay performed to determine appropriate seeding density and MTS incubation period for C6 cell line. Based on results a seeding density of 5,000 cells/well was chosen with a 3 hour MTS incubation for subsequent MTS assays regarding the C6 cell line.

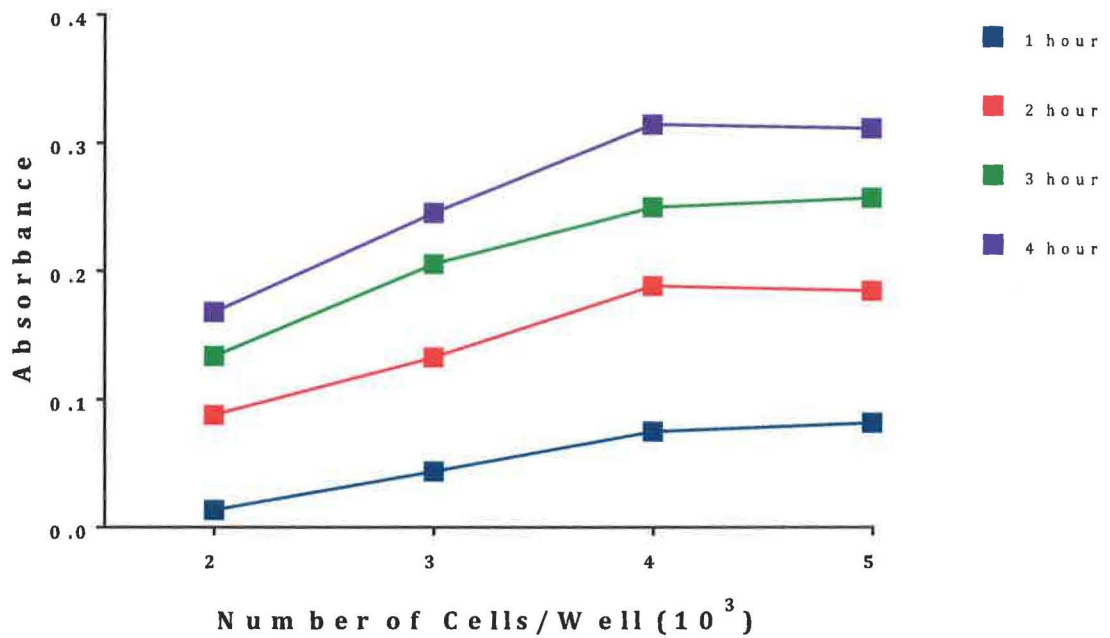


Figure 4: Metabolic curve for m-15 cell line. Preliminary MTS assay performed to determine appropriate seeding density and MTS incubation period for m-15 cell line. Based on results a seeding density of 5,000 cells/well was chosen with a 3 hour MTS incubation for subsequent MTS assays regarding the m-15 cell line.

Table 1. Seeding densities for each cell line and assay performed

<u>Assay</u>	<u>Seeding Vesicle</u>	<u>Cell Line</u>	<u>Density</u>
Phase Contrast Microscopy	24 well plate	SH-SY5Y	1,750 cells/well
Immunocytochemistry	4 well slide	SH-SY5Y	1,750 cells/well
MTS	96 well plate	SH-SY5Y	50,000 cells/well
		C6	5,000 cells/well
		m-15	5,000 cells/well

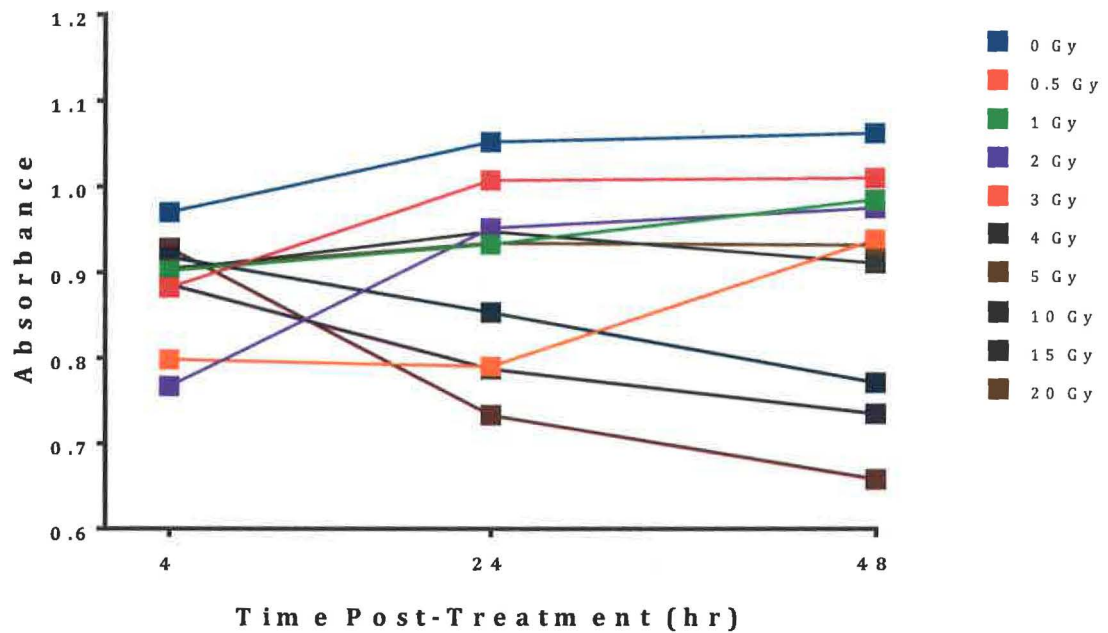


Figure 5: Preliminary x-ray radiation dose testing of SH-SY5Y cell line using MTS assay. A maximum dose of 20 Gy was used since absorbance was low (0.658) after 48 hours. Doses 0.5, 1, 2, 3, 4, and 5 Gy were similar in their absorbance at 48 hours and therefore 5 Gy was used. Based on data doses of 0, 1, 5, 10, and 20 Gy were chosen and used for MTS assay on all cell lines.

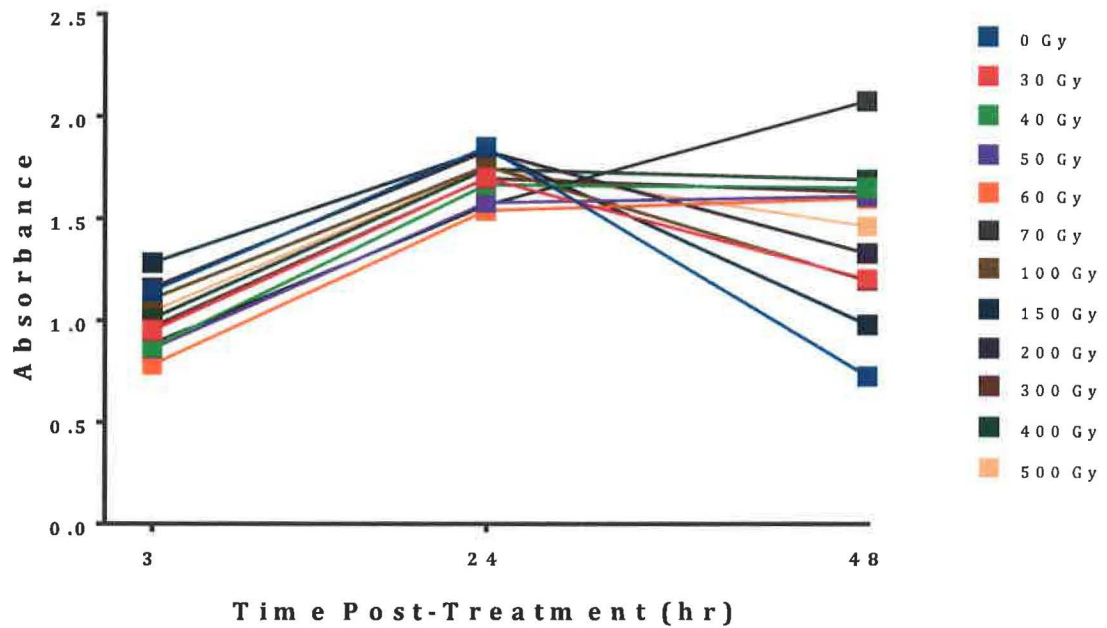


Figure 6: Additional x-ray radiation dose testing of C6 cell line. Since glial cells are thought to be more resistant to stress higher radiation doses were tested. All doses show the same trend where absorbance increases from 3 to 24 hours after treatment. Control cells not exposed to irradiation had an absorbance reading of 0.728 48 hours post treatment while all other doses had higher readings for the same time point.

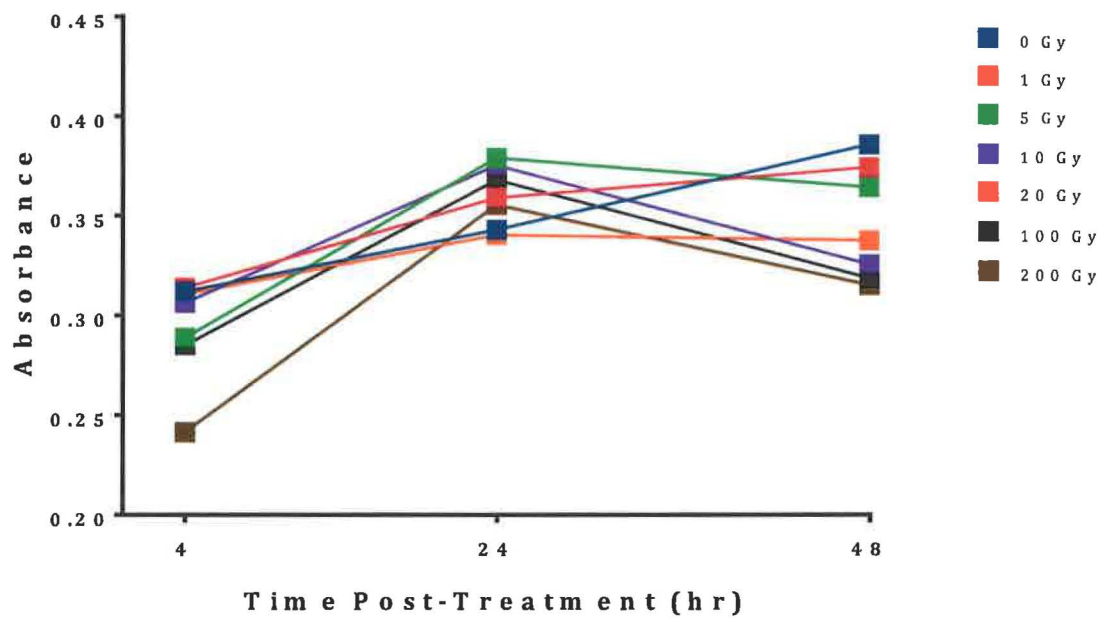


Figure 7: Additional x-ray radiation dose testing of m-15 cell line. All doses increased in absorbance from 4 to 24 hours post-treatment. Control and cells exposed to 1 Gy increased in absorbance from 24 to 48 hours while all other doses decreased in absorbance.

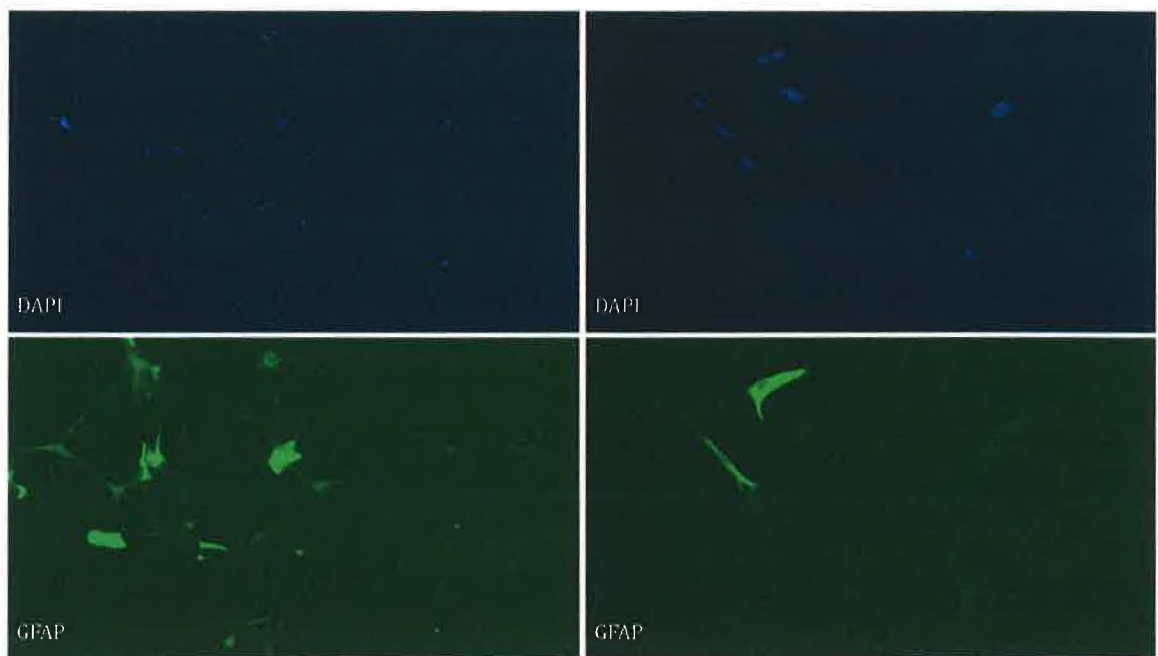


Figure 8: Representative images of glial fibrillary acidic protein (GFAP) staining of m-15 cell line. A portion of cells in the CL-mPG-15 cell line stained with Polyclonal Rabbit Anti-Glial Fibrillary Acidic Protein expressed GFAP. Left column is a representative image at 10X, right column 20X.

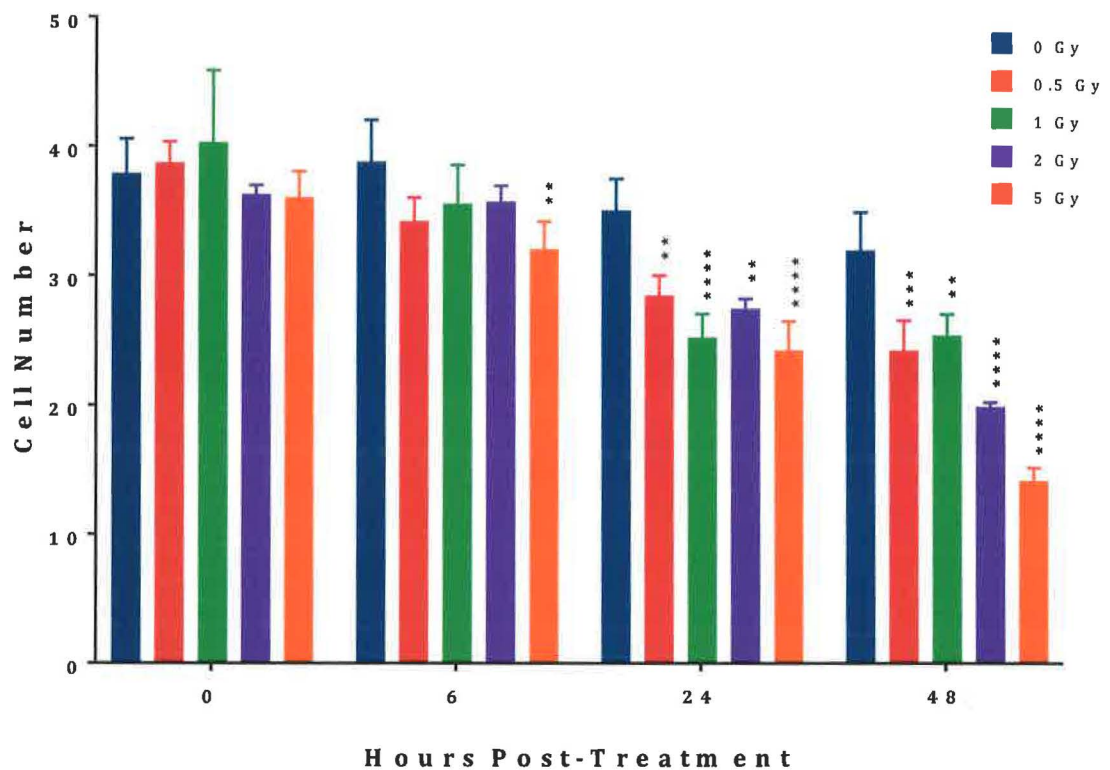


Figure 9: Cell number decreases in differentiated SH-SY5Y cells 24 and 48 hours post-treatment in response to increased x-ray radiation dose according to phase microscopy. Bars represent mean (n=3) \pm SEM where ** p<0.01, *** p<0.001, and **** p < 0.0001 relative to control (0 Gy at each time post-treatment) using two-way ANOVA and Dunnett's multiple comparisons test post hoc.

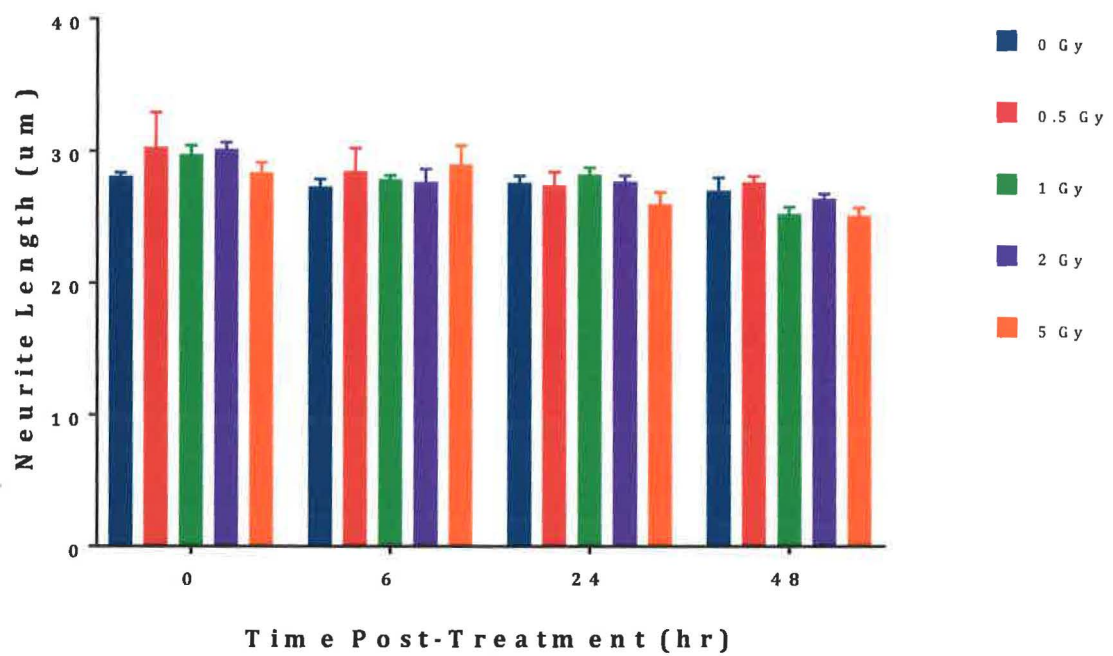


Figure 10: Neurite length does not change with increases in both dose and time post-treatment based on phase contrast microscopy. Bars represent mean (n=3) \pm SEM. Statistical test performed was two-way ANOVA and Dunnett's multiple comparisons test post hoc.

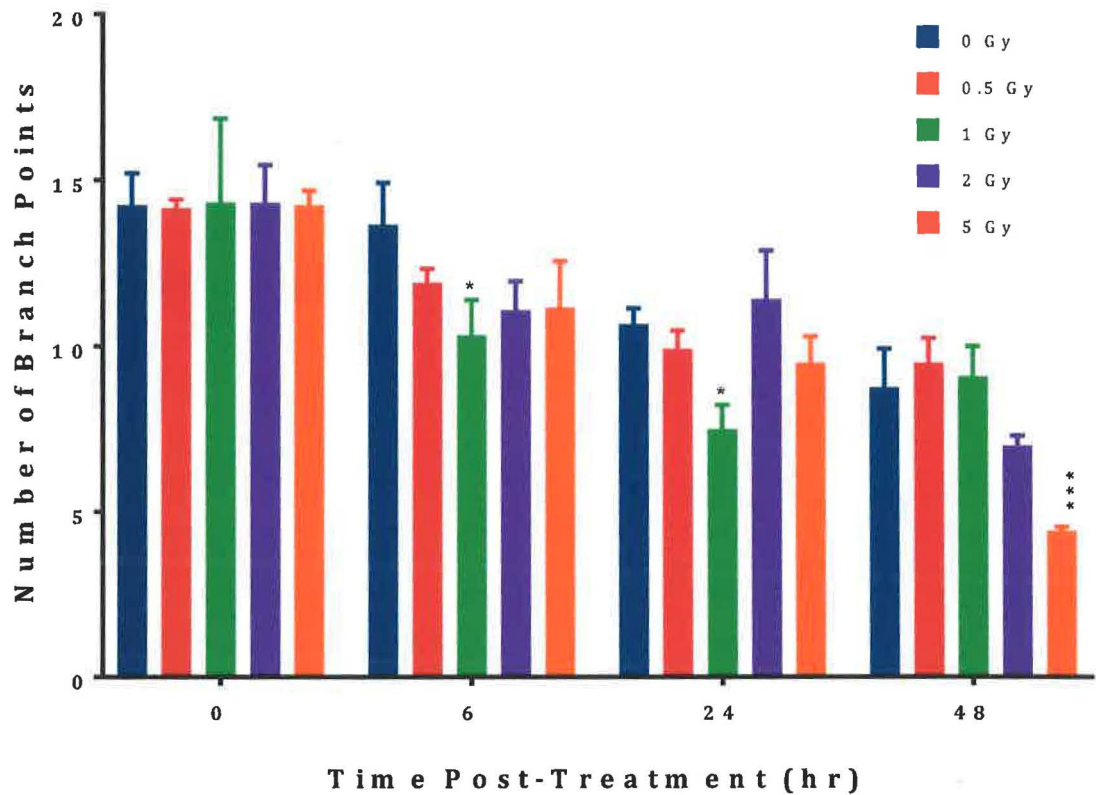


Figure 11: Number of branch points decrease in differentiated SH-SY5Y cells in select dose and time groups according to phase microscopy. Number of branch points was used as a way to monitor neurite complexity. Bars represent mean (n=3) \pm SEM where * $p < 0.05$ and *** $p < 0.001$ relative to control (0 Gy at each time post-treatment) using two-way ANOVA and Dunnett's multiple comparisons test post hoc.

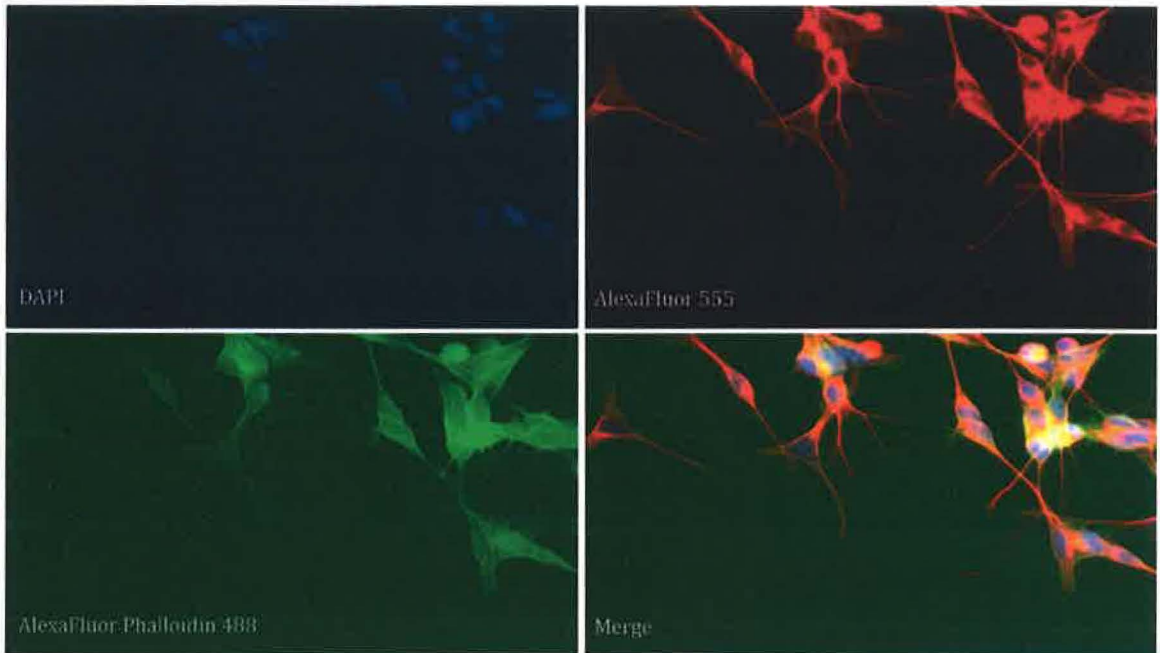


Figure 12: Representative images of immunocytochemistry staining for SH-SY5Y cell line at 20X magnification. Each image is the same field of view and therefore same cells. Top left: DAPI staining of nuclei, top right: AlexaFluor 555 staining of microtubules, bottom left: AlexaFluor Phalloidin 488 staining of actin, bottom right: merged image of all stains.

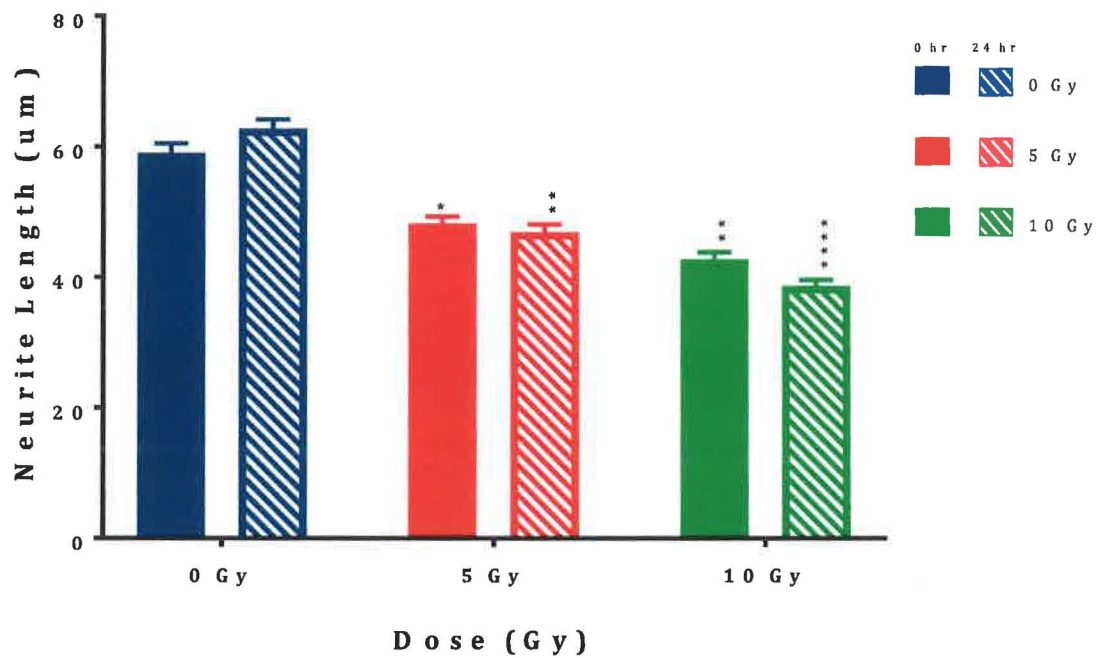


Figure 13: Neurite length of differentiated SH-SY5Y cells decreases in response to radiation dose and time post-treatment based on immunocytochemistry. Bars represent mean (n=3) \pm SEM where * $p < 0.05$, ** $p < 0.01$, and **** $p < 0.0001$ relative to control (0 Gy at each time post-treatment) using two-way ANOVA and Tukey's post hoc test.

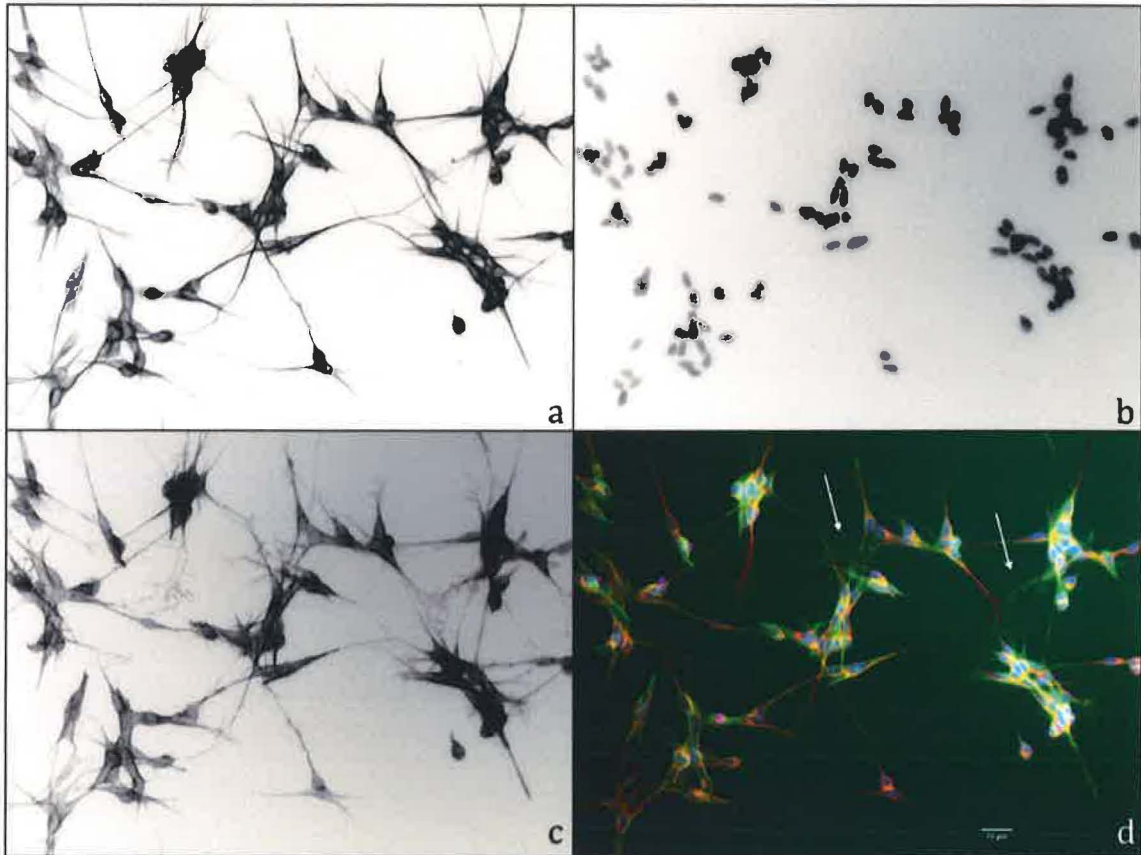


Figure 14: Control cells 48 hours post-treatment tend to exhibit complicated cytoskeleton structure. Microtubules are elongated and bundled (a), nuclei are present (b), and actin network is complex (c). White arrows in the colored merge (d) indicate areas of more complicated actin networking between cells. Scale bar represents 25 micrometers.

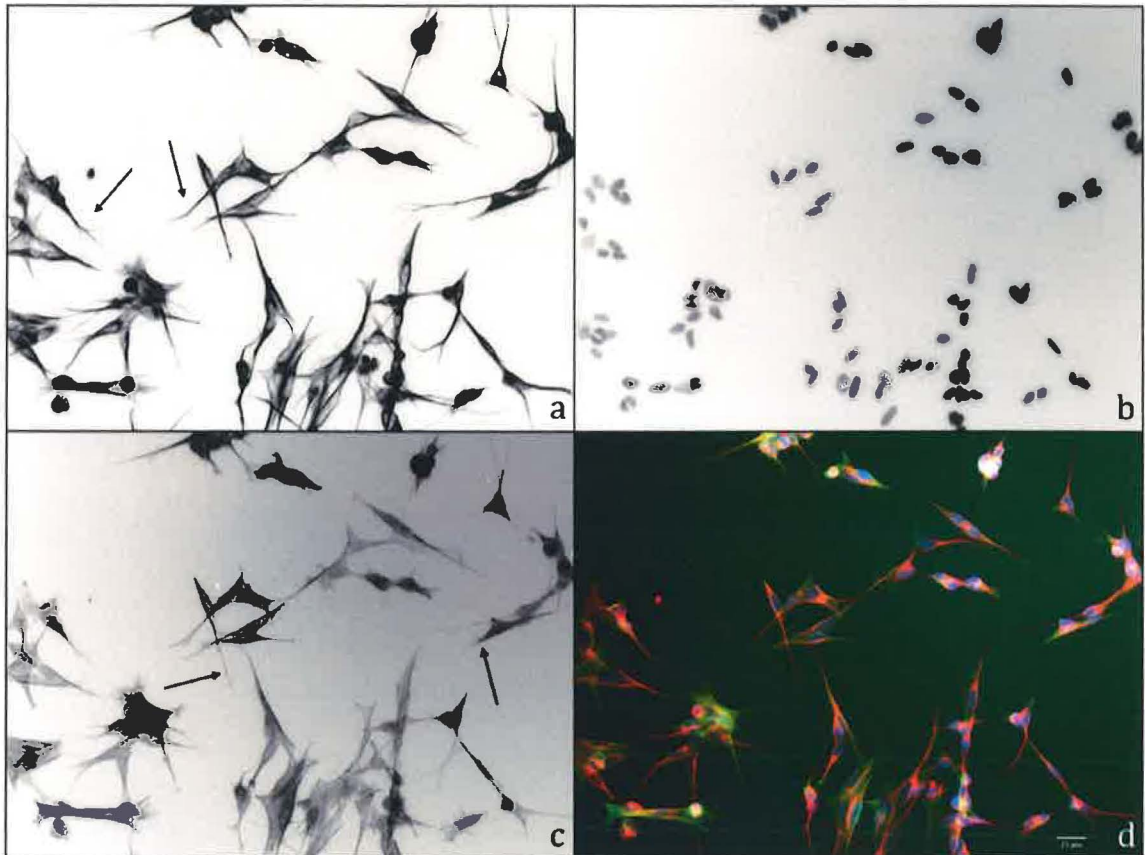


Figure 15: Treated SH-SY5Y cells possess the same overall cytoskeleton structure seen in control cells, although they tend to be shortened and less complex. Microtubules are bundled but not as lengthy (a), nuclei (b), actin networking is diminished; compare with white arrows in Figure 17 (d), (c), merge color image (d). Scale bar represents 25 micrometers.

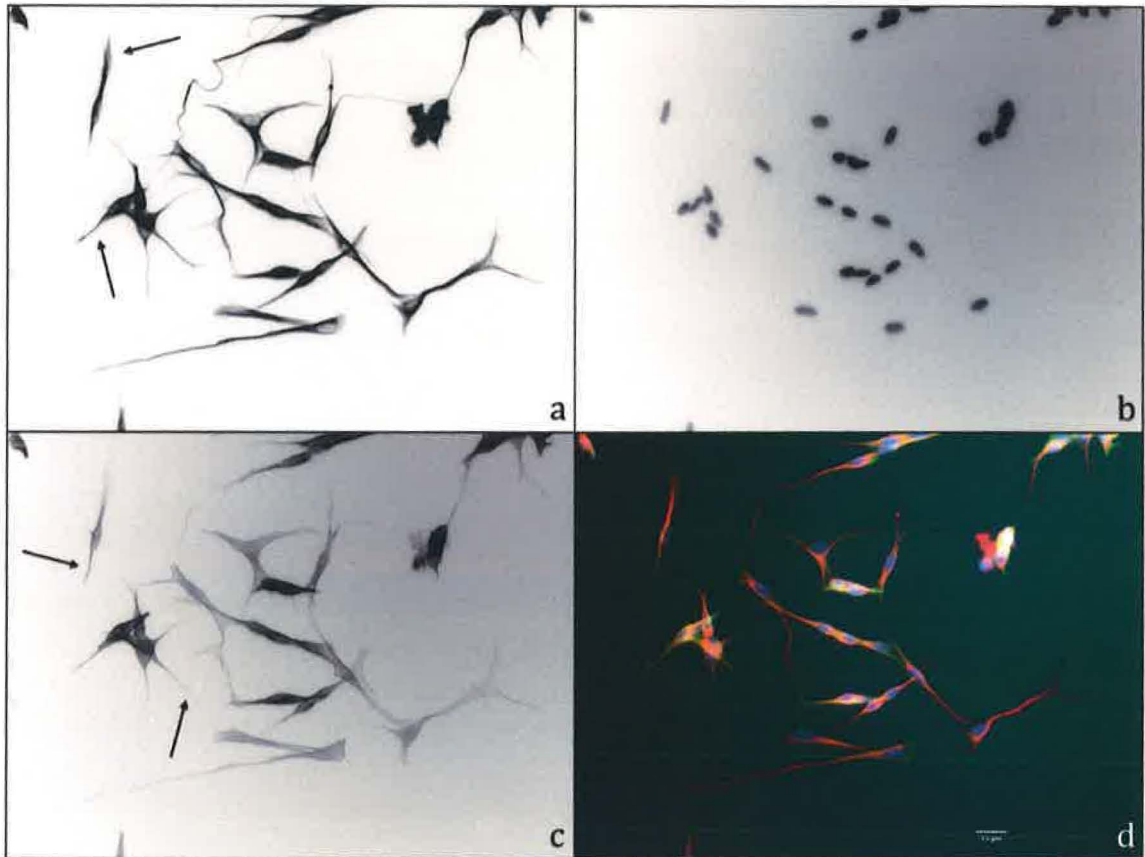


Figure 16: Not all control cells exhibit complex networking. Control cells can display shortened and/or loose microtubules (a) and diminished or absent actin structure (c). Nuclei are shown (b). Color merge Scale bar represents 25 micrometers.

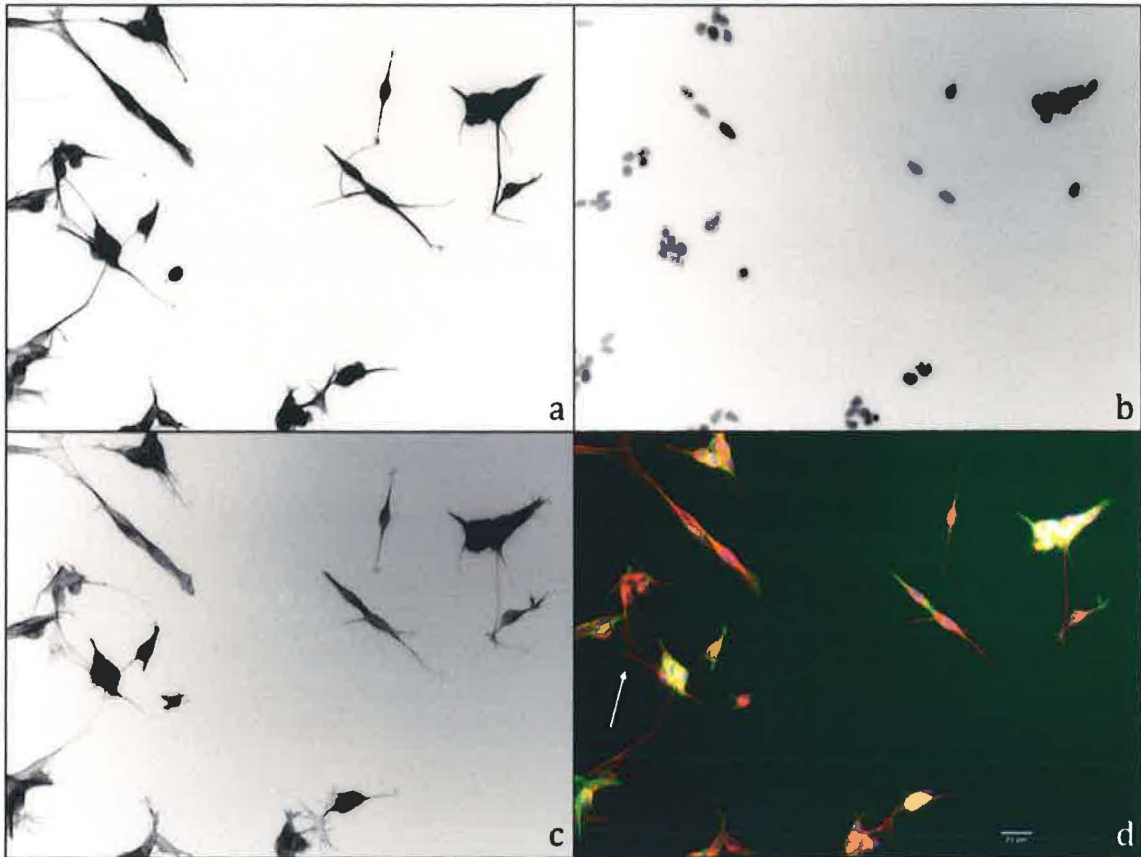


Figure 17: Treated SH-SY5Y cells can display complex neurites where microtubules are elongated (a) and actin structure is complex (c). Nuclei are shown (b). White arrows in color merge (d) show neurites with complicated networking seen in control cells. Scale bars represents 25 micrometers.

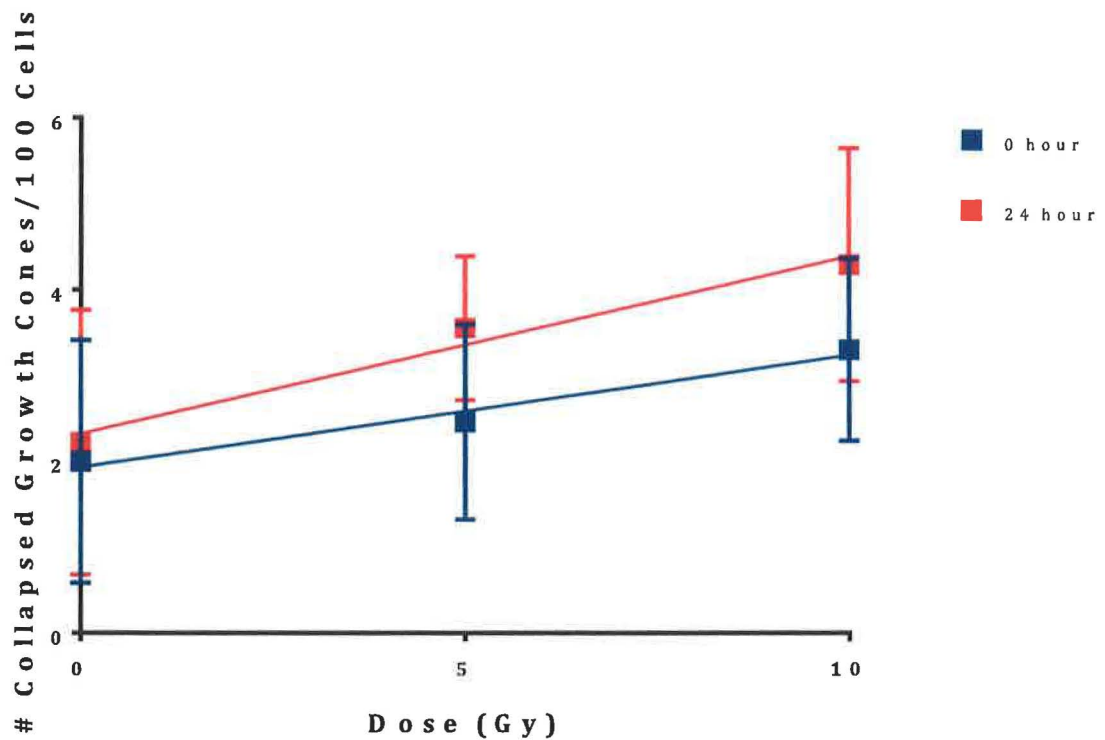


Figure 18: Number of collapsed growth cones does not change with dose or time (post-treatment) between SH-SY5Y control cells and x-ray treated cells. Data points represent mean ($n=3$) \pm SEM. Statistical test performed was two-way ANOVA and Dunnett's multiple comparisons test post hoc; no significant differences with dose or time were found.

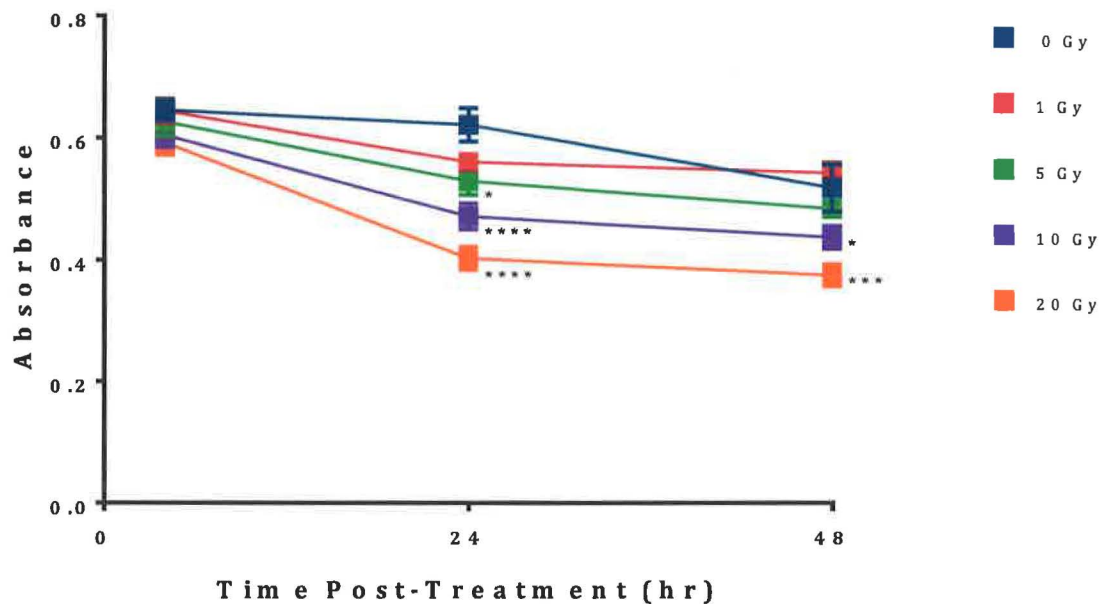


Figure 19: X-ray radiation causes a decrease in metabolic activity in SH-SY5Y cell line as determined by MTS assay. SH-SY5Y cells were exposed to 0, 1, 5, 10, and 20 Gy of x-ray radiation and metabolic activity analyzed after 0, 24, and 48 hours post-treatment. Absorbance decreased for all doses from 0 to 24 hours. Absorbance slightly increased for cells treated with 1 Gy from 24 to 48 hours while all other doses decreased in absorbance. Reported is the mean (n=3) \pm SEM where * p<0.05, *** p<0.001, and **** p<0.0001 relative to control (0 Gy at each time post-treatment) using two-way ANOVA and Dunnett's multiple comparisons test post hoc.

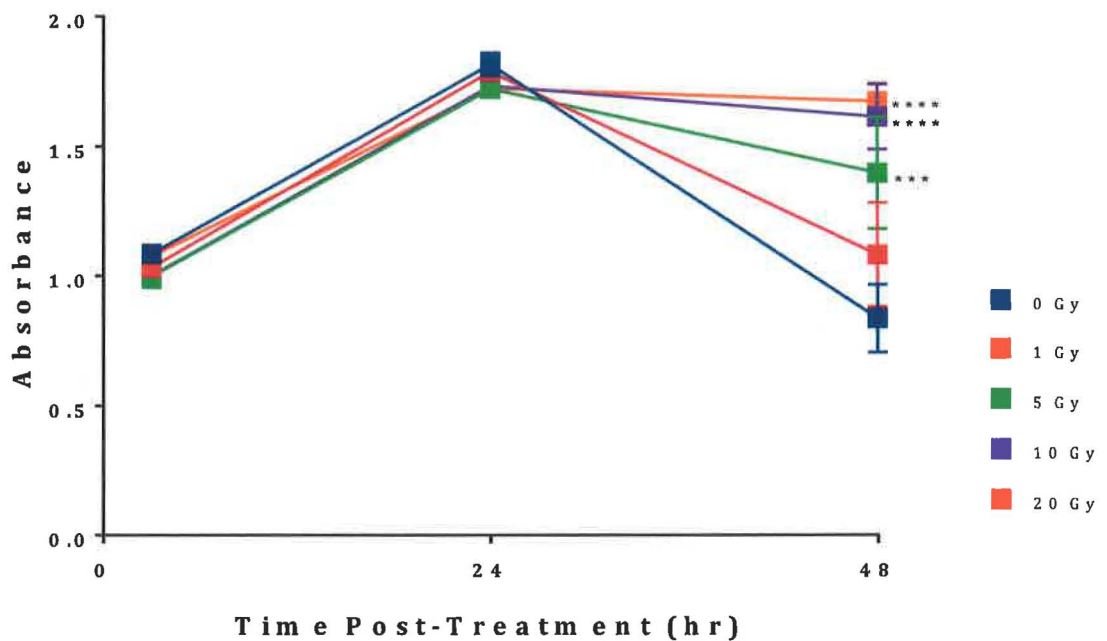


Figure 20: X-ray radiation causes an increase in metabolic activity 48 hours post-treatment in the C6 cell line as determined by the MTS assay. C6 cells were exposed to 0, 1, 5, 10, and 20 Gy of x-ray radiation and metabolic activity analyzed after 0, 24, and 48 hours post-treatment. All doses increased in absorbance from 0 to 24 hours but decreased from 24 to 48 hours. Reported is the mean (n=3) \pm SEM where *** p<0.001 and **** p<0.0001 relative to control (0 Gy at each time post-treatment) using two-way ANOVA and Dunnett's multiple comparisons test post hoc.

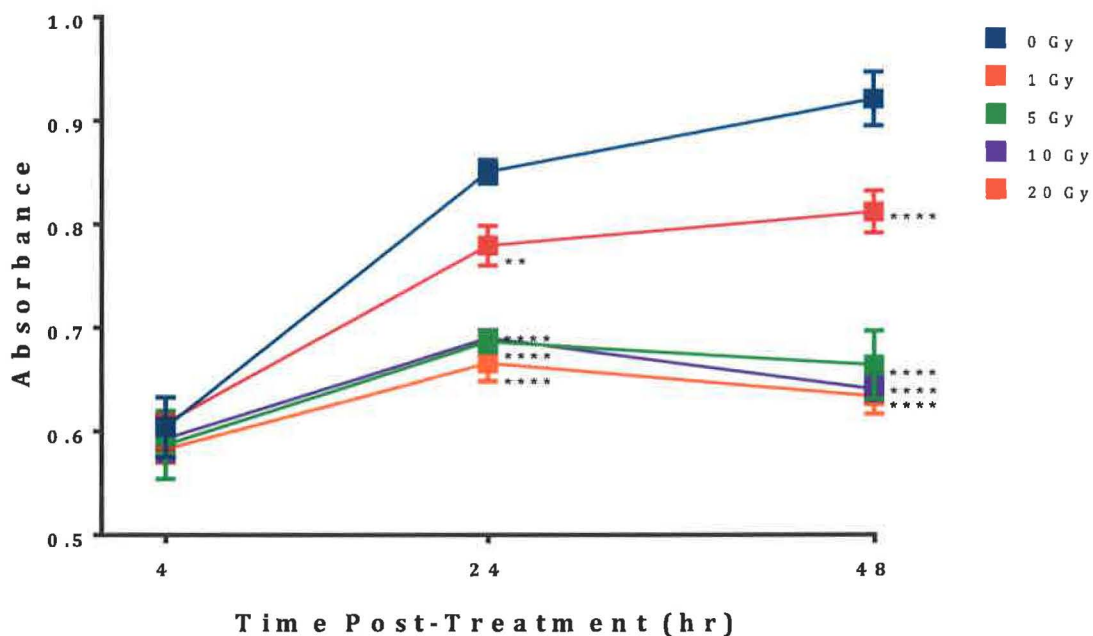


Figure 21: X-ray radiation causes a decrease in metabolic activity in the m-15 cell line as determined by the MTS assay. m-15 cells were exposed to 0, 1, 5, 10, and 20 Gy of x-ray radiation and metabolic activity analyzed after 0, 24, and 48 hours post-treatment. All doses increased in metabolic activity from 0 to 24 hours. Doses of 0 and 1 Gy showed increases in absorbance from 24 to 48 hours while all other doses decreased. Reported is the mean (n=3) \pm SEM where ** p<0.01 **** p<0.0001 relative to control (0 Gy at each time post-treatment) using two-way ANOVA and Dunnett's multiple comparisons test post hoc.

4: DISCUSSION

4.1 GENERAL DISCUSSION

4.1.1 Preliminary Experiments (seeding density and dose testing)

The purpose of this study was to determine the effects of x-ray radiation on neurite morphology and cytoskeleton structure using the well-studied SH-SY5Y cell line. Additionally, we examined radiation's effects on both cancerous and primary glial cell lines since, until recently, these cells have been ignored.

Preliminary dose testing was done in order to establish which radiation doses would yield cytotoxic effects and which could be used in all subsequent experiments. SH-SY5Y cells were used in these dose testing experiments to model neurons. Neurons are more sensitive than glial cells to oxidative stress (Ben-Yoseph et al. 1994), which is one consequence of radiation exposure and glial cells play a role in protecting neurons against oxidative stress (Iwata-Ichikawa et al. 1999). Because of this, it is reasonable to infer that higher exposures to radiation would be more cytotoxic to neurons than to glial cells; and in order to observe the effects of radiation the neuronal cell line would have to be the basis for all experiments.

Immunocytochemistry staining for GFAP (as shown in Figure 8) confirmed the CL-mPG-15 cell line was glial in origin. Glial fibrillary acidic protein is a component of astrocyte cytoskeletons and has proven useful in identifying astrocytes (Reske-

Nielsen et al. 1987). In our study, there were two clear populations of cells after staining. One population fluoresced strongly while the other exhibited a weak signal. This weak signal could be low levels of GFAP staining or simply background fluorescence. While our CL-mPG-15 cell line contains astrocytes, we cannot be certain it does not contain other cells of the central nervous system. Further testing could be done in order to identify what other cell populations exist with known astrocytes in the CL-mPG-15 cell line. It is possible that different cell types would respond differently to radiation exposure.

4.1.2 Effects of Radiation on Differentiated SH-SY5Y Morphology

Phase contrast microscopy shows cell number decreases in differentiated SH-SY5Y cells over time with increased x-ray radiation dose. This is an expected result since radiation is known to be cytotoxic (National Research Council 2006; Stickel et al. 2014). Changes in nervous system tissue has been seen in multiple studies where both low (0.25-1 Gy) and high (up to 10 Gy for x-ray and 60 Gy for alpha particles) doses of ionizing radiation are used (Betlazar et al. 2016). Neurite complexity has been measured in previous studies by counting number of branch points and the length of the neurite (Radio and Mundy 2008). Phase imaging also revealed that SH-SY5Y neurite complexity decreased in cells exposed to 1 Gy radiation at 6 and 24 hours' post-treatment and 5 Gy 48 hours post-treatment. All other doses and time points were not significantly different from control cells. Lastly, phase contrast microscopy indicates that neurite length does not change with either dose or time. Length, for this study, is defined as the longest neurite for each discernible soma

which is common practice in quantifying neurite outgrowth (Harrill et al. 2013; Das et al. 2004; Radio and Mundy 2008). In our study neurite length was used as a tool to reveal the occurrence of neurite retraction, where neurite length decreases in response to unfavorable conditions like exposure to toxicants. Proper function of the nervous system is reliant on maintaining connections with post-synaptic partners. If radiation causes retraction of neurites, then this would result in reduced circuit function as connections would be lost after retraction. Full CNS function is critical for astronauts as they are required to complete complex tasks and think critically and quickly. Lives of astronauts as well as costly missions could be at risk if neurite retraction and reduced function associated with it occur. While this will affect small numbers of astronauts that may travel beyond Earth's protective magnetic field, these consequences will also affect the growing number of individuals receiving medical testing that utilizes radiation for diagnostics as well as cancer patients receiving radiation therapy.

Our hypotheses were that neurite complexity and length would decrease with time for all radiation doses. While immunocytochemistry results suggest neurite length decreases with radiation dose, phase imaging was contradictory in showing no change in neurite length. There are logical reasons for such unexpected results. Despite seeding 1,750 SH-SY5Y cells per well, only a very small subset of cells were actually examined. In each well only one of 8 possible quadrants were imaged and analyzed. Additionally, one criteria for choosing a quadrant was based on how spaced SH-SY5Y cells were. This selection allows for ease and accuracy when

tracing, since neurites can't be analyzed if cells are clustered and neurites overlap. Future data may differ if a larger sample of cells are analyzed. Inexperience could also explain our unanticipated results. Examining and tracing neurites is a complicated process. Enlarging an image and adjusting parameters such as contrast and brightness in ImageJ software may allow for visualization of extended neurites not initially visible. Focusing and enlarging one area of an image allows you to see neurites more accurately while adjusting brightness and contrast allows for detection of thinner neurites, which are hard to detect otherwise. Despite training, it's possible that a more experienced analyzer would yield different results.

4.1.3 Effects of Radiation on SH-SY5Y Cytoskeleton Structure

A functional nervous system is dependent on precise pathfinding, the ability of a neuron to send its axon to the proper destination. This requires dynamic interactions between cytoskeletal components, actin and microtubules (Geraldo and Gordon-Weeks 2009; Lowery and Van Vactor 2009). The cytoskeleton of neurites plays an equally important role in maintaining axon structure and integrity in developed nervous tissues. In fact, compromised cytoskeleton structure has been linked to both neurodevelopment *and* neurodegenerative diseases (Kevenaar and Hoogenraad 2015; Kirkpatrick and Brady, 1999). Any disruption in actin and microtubule structure could be detrimental to the organism since neuronal function is dependent on proper structure and synaptogenesis. Thus, disruption to cytoskeletal structure is an important aspect of neurotoxicology.

Immunocytochemistry was used to evaluate effects of x-ray radiation on

cytoskeleton organization in the SH-SY5Y cell line where neurite length and number of collapsed growth cones were analyzed.

In opposition to phase contrast microscopy results, immunocytochemistry revealed neurite length of differentiated SH-SY5Y cells decreases with radiation dose and time. This difference in results is puzzling and likely from experience of the analyzer. Perhaps increased sensitivity of immunocytochemistry reveals finer details of cytoskeleton structures making visualization and tracing easier resulting in more accurate results. Again, neurite retraction could cause neurodegeneration and deficiency in nervous system function.

One obvious discrepancy within our data brings forth the question, why do phase image microscopy and immunocytochemistry yield different neurite length results? How does phase imaging suggest neurite length does not change with either increases in x-ray radiation dose or time while immunocytochemistry suggests the opposite? The only difference between the two assays were the cell culture vessels in which they were seeded; number of cells seeded into each remained constant. For phase contrast microscopy, cells were seeded into 24 well plates (1,750 cells/1.9 cm²) while 4 well chamber slides (1,750 cells/1.7 cm²) were used for immunocytochemistry. Reflecting on these results led to correspondence with a representative from Faxitron, the company that manufactures the x-ray cabinet system. The thought was that the two assays resulted in different conclusions due to differences in: type of plastic between assay plates/slides, thickness of plastic,

volume of media and cell densities adhered to vessels. All of which could alter the amount of radiation delivered to cells.

Discussion with the Faxitron representative confirmed that the x-ray beam can be greatly affected by the type of vessel in which cells are seeded; although it is not clear exactly to what degree each plastic type would alter x-ray quality or quantity. Many studies have been done to evaluate percentage depth dose (PDD), the dose of beam radiation that is absorbed through a medium at any given depth. PDD can be calculated and is analyzed by comparing decreases in beam intensity in comparison to its initial intensity. Increases in PDD decrease radiation dose absorbed by cells (Memon et al. 2015). Both the 24 well plates and 4 well slides have equal amounts of volume, 500 uL. However, the 24 well plates have a slightly larger surface area than the 4 well slides (1.9 cm² and 1.7 cm², respectively). This would lead us to think that if neurite growth decreased it would more than likely be in the phase imaging results where surface area is larger and therefore the media column is less deep . The fact that it was seen via immunocytochemistry instead is puzzling. More studies should be done to investigate. Yet, intuitively it makes sense that a thicker or more dense plastic, as well as deeper volume of media would cause more dose attenuation and therefore less measurable effects in cells. Perhaps the vessel plays a more important role than originally thought. (Robert Hase, email correspondence sent to author, October 7, 2016; November 11, 2016; November 14, 2016, December 2, 2016).

In addition to neurite length, number of collapsed growth cones was assessed. Statistical analysis reveals no difference in number of collapsed growth cones with either dose or time. However, there is a trend that collapsed growth cone number increases with radiation dose and time. Statistical insignificance can result from the timing of growth cone collapse and from large variability in the data due to ambiguous definitions of what constitutes a collapsed growth cone. If any actin was observed in the tip of the neurite or growth cone, it was *not* considered collapsed. Such strict guidelines presumably excluded growth cones that were collapsed or collapsing. Future analysis should set a more refined definition of a collapsed growth cone. Perhaps analytical software like ImageJ can provide a mask that allows the operator to separate collapsed from non-collapsed growth cones by use of fluorescence readings in a set area. If a growth cone has less area than that defined by the operator, it would be considered collapsed. The variability in size of growth cones in SH-SY5Y cells also adds to the difficulty. Despite non-significant results these immunocytochemistry images can be reviewed and re-analyzed at a later time and may yield different results if we can define a more sophisticated assay.

4.1.4 Cytotoxicity of Radiation

MTS Assay is a tool to measure metabolic activity. Decreases in metabolic activity are presumed to be due to cell death thereby making the MTS Assay a tool to measure cytotoxicity. X-ray radiation is cytotoxic to SH-SY5Y cells. This is not surprising as radiation is known to cause oxidative stress ([Morgan et al. 1996](#)) and

neurons are more sensitive to radiation than other cells of the nervous system (Ben-Yoseph et al. 1994).

Clear differences in metabolic activity can be seen in the C6 cell line in comparison to SH-SY5Y cells. In C6 cells after treatment with radiation, metabolic activity first increased from 0 to 24 hours for all doses then decreased in a dose dependent manner from 24 to 48 hours where higher doses showed little differences in metabolic activity and control cells showed the most significant decreases in metabolic activity. This was a surprising outcome. Since the C6 cell line is glial in origin, it is possible that control cells continued to divide from 0 to 24 hours post-treatment and ceased or slowed division from 24 to 48 hours. This would explain diminished metabolic activity. Our initial thoughts on higher metabolic activity with higher doses at 48 hours post-treatment were that treated cells could be ramping up DNA repair mechanisms-which are metabolically demanding. However, upon visual inspection, it appeared that as dose increased so did the cell number. This would mean that x-ray radiation causes cell division of C6 cells and possibly other glial cells.

Cancer treatment is involved and tailored for each patient depending on a variety of factors. Johns Hopkins Medicine states that radiation is used to treat gliomas after surgery, when surgery is not a viable option due to the location of the tumor, or to treat gliomas that have returned (Johns Hopkins Medicine). If our results are true, gliomas being treated with radiation could cause division of cancer cells and be

more detrimental to the patient. Despite this, caution must be used when extrapolating our results since the C6 cell line was established nearly 50 years ago; our cells may not act like earlier generations of the same cell line.

In order to further investigate increases in metabolic activity in both glial cell lines in response to x-ray radiation, Hoechst staining was used in order to stain nuclei and count cells. However, Hoechst staining was too faint to analyze-likely due to age of the stain. Testing was supposed to resume; however, a yellow oil was seen inside the Faxitron x-ray cabinet. It was determined that transformer oil was leaking from the HV transformer and x-ray tube housing tub. Due to the high cost to repair the Faxitron cabinet, further testing with x-ray radiation was not conducted.

Despite these setbacks, future testing on cell division of glial cells and gliomas upon exposure to radiation is something that needs to be examined. If in fact radiation causes cell proliferation in gliomas, unintended and detrimental side effects could result in patients treated for these types of cancer. This is not the only concern of radiation use in the medical setting.

Advances in technology have allowed for more powerful diagnostic tools available to physicians and the like. These tools, however, expose patients to large doses of radiation. Computed tomography (CT) or computerized axial tomography (CAT) is a medical imaging procedure where x-ray radiation is used to create detailed 3-dimensional images/scans of tissue, bone, blood vessels, organs, etc. (National

Cancer Institute). Since its invention in the early 1970's, the use of CT scans has increased dramatically. In 1980, 3 million CT scans were performed compared to 65 million in 2002.

Between the mid 1980's and 1990's there was a 500% increase in the use of CT scans; and in 2007 it was estimated that 13% of all diagnostic imaging procedures were from CT scans alone (Brenner and Hall 2007; Voress 2007). The rise in CT is attributed to its many benefits. The procedure is quick, noninvasive, and gives physicians better images in order to more accurately diagnose patients. CT scans are also more cost effective than other medical imaging techniques, like magnetic resonance, especially when patients have insurance. It is thought that physicians are using CT scans as a "defensive medicine" where superfluous scans are performed in an attempt to accurately diagnose patients and avoid malpractice lawsuits (Voress 2007). Despite their many benefits, CT scans expose patients to far more radiation than most other medical imaging techniques. For comparison, one abdominal CT scan is the equivalent of receiving 500-1000 chest x-rays one after another (Lee et al. 2004; Robb 2004; Voress 2007). It is estimated that up to 2% of cancer within the US may be due to excessive use of CT scans (Brenner and Hall 2007; Samson 2008).

Perhaps the most alarming concern about CT scans is the seeming inability of emergency room physicians and radiologists to accurately estimate their radiation doses. Lee et al. (2004) published a study where emergency room physicians and radiologists were surveyed in order to assess their awareness of radiation dose and

potential risks attributed to CT scans. They found that 53% of radiologists and 91% of emergency-room doctors did not believe that CT scans were associated with increased cancer risk; and 75% of both are not only unable to accurately estimate doses of radiation patients are being exposed to with this type of imaging but grossly underestimated CT scan radiation dose (Brenner and Hall 2007; Lee et al. 2004).

Proper use of radiation within the medical setting is imperative. Physicians should be aware of radiation doses of CT and risks involved; benefits should outweigh the risks when ordering CT scans and care should be taken to not unnecessarily expose patients to them. Excessive use of CT scans can potentially cause damage to the nervous system and initiate carcinogenesis; we must use it with caution as to not cause more radiation exposure than necessary.

4.2 FUTURE AIMS

4.2.1 General

Despite noteworthy outcomes from this study, more research needs to be done to answer additional questions that arose. Cells lines like the glial C6 and SH-SY5Y neuronal cell lines are useful tools. However, because of their cancerous origins they are not ideal and may not reflect behavior or circumstances of primary cells or cells *in vivo*. Therefore, primary neurons should be used to determine their response to x-ray irradiation in order to compare against SH-SY5Y cells. To further mimic the *in vivo* environment, co-culturing of neurons and glia is critical. Until recently, glial

cells have largely been ignored and their importance underestimated. In order to understand how neurons and glia behave to a toxin/toxicant it is imperative we figure out how these cells interact. The Currie Laboratory is currently investigating microfluidics and will likely produce a co-culturing device to perform these studies.

Additionally, it would be beneficial to perform these experiments using particle radiation. We could then correlate space radiation to the deficits seen during and after exposure to GCR creating a more realistic environment of astronauts traveling beyond LEO. This is unlikely as our lab is small and doesn't have the funding or notoriety to gain time on particle accelerators. This doesn't mean this study was for naught. In fact, it is relevant on a larger scale as there are far more people exposed to man-made radiation (like x-rays) for medical testing and radiation therapy than there are astronauts exposed to GCR. Therefore, it is critical that we figure out the long-term effects of radiation therapy to better treat those affected and limit exposure if need be.

4.2.2 Reducing Effects of Radiation

4.2.2.1 Nutraceuticals

Oxidative stress has been linked as a possible mechanism to the aging process as well as neurodegenerative diseases like Alzheimer's Disease (Kelsey et al. 2010; Lin and Beal 2006; Martin and Grotewiel 2006; Nunomura et al. 1999; Nunomura et al. 2001). Mitochondria are the primary source of oxidative stress. Mitochondria generate cellular energy in the form of ATP through oxidative phosphorylation and

the electron transport chain (ETC). Despite their ability to create ATP efficiently, leakage of electrons is inevitable and their reaction with molecular oxygen creates reactive oxygen species and free radicals (Kelsey et al. 2010; Lee et al. 2004).

Radiation not only causes production of reactive oxygen species but also exacerbates leakage by the electron transport chain within mitochondria (Azzam et al. 2012; Lee et al. 2004). Without intervention, oxidative stress causes damage to proteins, lipids, and DNA. It is the oxidative damage to cellular proteins and build-up of these dysfunctional proteins that lead to neurodegenerative disorders (Linseman 2009).

One promising strategy for mitigating oxidative stress is using natural dietary supplements termed, nutraceuticals. Nutraceuticals are antioxidants that reduce reactive oxygen species and free radicals thereby decreasing oxidative stress. (Calabrese et al. 2008; Kelsey et al. 2010; McCarty 2006; Schaffer et al. 2012). Many nutraceuticals act as neuroprotective agents and are potential therapeutic agents for neurodegenerative disorders. These antioxidants include: flavonoid polyphenols (like EGCG found in green tea and quercetin), non-flavonoid polyphenols (curcumin and resveratrol), phenolic acids and diterpenes (rosmarinic and carnosic acids), and organosulfur compounds (allicin and L-sulforaphane). A number of these antioxidants not only decrease free radicals but also modulate pro-survival or pro-apoptotic signaling pathways, bolstering their therapeutic potential (Kelsey et al. 2010).

Nutraceuticals have been termed as “functional foods” or “medicinal foods.” They are becoming increasingly popular in the United States as the benefits of these antioxidant foods becomes more widespread. Many fruits, vegetable, spices, herbs, teas and wines contain antioxidants and are considered nutraceuticals. Easy accessibility make these medicinal foods a good choice to incorporate into diets of astronauts as well as patients undergoing radiation therapy in an attempt to lessen negative impacts of radiation exposure.

4.2.2.2 Erythropoietin (EPO)

Erythropoietin (EPO) is another candidate for reducing the effects of radiation. Erythropoietin is a cytokine that stimulates erythropoiesis, or red blood production and increases oxygen supply to tissues. Like many other biomolecules, erythropoietin was long thought to have only one function. However, it likely serves other functions since EPO and erythropoietin receptors (EPOR) are present in neuronal tissues (Sakanaka et al. 1998) and since EPO is produced by both astrocytes and neurons (Juul et al. 1998). In fact, neurodevelopment may be dependent on the EPO/EPOR system since expression of both changes significantly during development of the brain (Buemi et al. 2003).

Due to its ability to increase oxygen supply, it is not surprising that EPO has been found to protect neurons against ischemic injury and is a promising therapeutic agent for stroke patients (Ehrenreich et al. 2002; Sakanaka et al. 1998; Zhang et al. 2010). In addition, EPO is thought to be involved in many cellular processes related

to tissue protection and damage repair including: protect against oxidative stress, reduce neuroinflammation, preserving/restoring blood-brain barrier integrity, promotes neuronal differentiation (even in adults), stimulates regrowth of axons, formation of neurites, dendritic sprouting, and electrical activity, and regulates intracellular calcium as well as the synthesis and release of neurotransmitters (Byts and Sirén 2009). Studies where erythropoietin alpha was systemically administered shows that EPO is anti-apoptotic and protects against hypoxia-induced glutamate toxicity, an excitotoxicity that causes nerve cell damage or death (Brines et al. 2000; Buemi et al. 2003; Lykissas et al. 2007; Morishita et al. 1997); reduces immune response and inflammation (Agnello et al. 2002; Brines 2002; Lykissas et al. 2007); protects against brain injury, like concussions (Brines et al. 2000), and helps maintain the integrity of the blood-brain barrier by protecting against VEGF-induced permeability (Martínez-Estrada et al. 2003).

As previously mentioned, radiation can cause neuronal apoptosis, demyelination of nerve fibers, oxidative stress and ultimately neuroinflammation and neurodegeneration. Studies are already underway to examine EPO's therapeutic use. One such study found that endogenous EPO prevented axonal degeneration and that nitric oxide is the signal that triggers production of EPO from glial cells upon axonal injury (Keswani et al. 2004).

Despite its therapeutic potential, one of the biggest challenges hindering the use of EPO is its inability to cross the blood-brain barrier (BBB) at clinically relevant levels.

Only about 0.5-1% of EPO administered systemically crosses the BBB (Brines and Cerami 2005; Zhang et al. 2010). In order to achieve therapeutic levels in nervous tissue, such large amounts of EPO would have to be administered that it could be harmful, causing polycythemia (elevated red blood cell count) and secondary stroke (Brines et al. 2000; Ehrenreich et al. 2002; Zhang et al. 2010). For this reason, more recent studies aim to enhance delivery of EPO across the blood-brain barrier. Elevated EPO levels in the brain were achieved by two groups that both created fusion proteins. Zhang et al. fused EPO with protein transduction domain derived from HIV TAT (Zhang et al. 2010). Boado et al. created an IgG molecular Trojan horse by fusing EPO to the carboxyl terminus of the IgG heavy chain (Boado et al. 2010).

Perhaps with more research, we can find a way to use EPO both pre- and post-space travel as well before and after radiation treatment to help reduce or prevent negative effects associated with radiation.

5: CONCLUSION

Undoubtedly, space exploration is fascinating and beneficial for mankind. In order for NASA to allow future space missions that would expose astronauts to dangerous radiation encountered beyond LEO we must understand the hazards and potential long-term effects. Although space travel is important, the number of astronauts that will be exposed to GCR pales in comparison to the population of those exposed to

radiation from medical diagnostics and cancer treatment. Care needs to be taken in order to understand the potential long-term effects of radiation on the nervous system in order to protect patients and mitigate possible health risks associated with such medical practices.

6: REFERENCES

Agholme, L., Lindström, T., Kågedal, K., Marcusson, J., & Hallbeck, M. (2010). An in vitro model for neuroscience: differentiation of SH-SY5Y cells into cells with morphological and biochemical characteristics of mature neurons. *Journal of Alzheimer's Disease*, 20(4): 1069-1082.

Agnello, D., Bigini, P., Villa, P., Mennini, T., Cerami, A., Brines, M.L., & Ghezzi, P. (2002). Erythropoietin exerts an anti-inflammatory effect on the CNS in a model of experimental autoimmune encephalomyelitis. *Brain Research*, 952(1): 128-134.

Amberger, V.R., Hensel, T., Ogata, N., & Schwab, M.E. (1998). Spreading and migration of human glioma and rat C6 cells on central nervous system myelin in vitro is correlated with tumor malignancy and involves a metalloproteolytic activity. *Cancer Research*, 58(1): 149-158.

American Brain Tumor Association. (2014). Brain Tumor Statistics. Accessed March 16, 2016. <http://www.abta.org/about-us/news/brain-tumor-statistics/>.

Anderson, J.L., Mertens, C.J., Grajewski, B., Luo, L., Tseng, C.Y., & Cassinelli, R.T. (2014). Flight attendant radiation dose from solar particle events. *Aviation, Space, and Environmental Medicine*, 85(8): 828-832.

Asaithamby, A., Uematsu, N., Chatterjee, A., Story, M.D., Burma, S., & Chen, D.J. (2008). Repair of HZE-particle-induced DNA double-strand breaks in normal human fibroblasts. *Radiation Research*, 169(4): 437-446.

Aschner, M. (1994). Bilirubin and Other Brain Cells. *Pediatrics*, 93(1): 155-156.

Association of Flight Attendants-CWA and Department of Air Safety, Health & Security. (Updated April 2010). Cosmic and Solar Radiation: Facts for Flight Attendants. Accessed April 2016. <http://ashsd.afacwa.org/docs/radbroch1.pdf>.

Azzam, E.I., Jay-Gerin, J.P., & Pain, D. (2012). Ionizing radiation-induced metabolic oxidative stress and prolonged cell injury. *Cancer Letters*, 327(1): 48-60.

Baes, F. (2015). Health Physics Society. Accessed April 8, 2015. <http://hps.org/>.

Barcellos-Hoff, M.H., Park, C., & Wright, E.G. (2005). Radiation and the microenvironment—tumorigenesis and therapy. *Nature Reviews Cancer*, 5(11): 867-875.

Ben-Yoseph, O., Boxer, P.A., & Ross, B.D. (1994). Oxidative stress in the central nervous system: monitoring the metabolic response using the pentose phosphate pathway. *Developmental neuroscience*, 16(5-6): 328-336.

- Benda, P., Lightbody, J., Sato, G., Levine, L., & Sweet, W. (1968). Differentiated rat glial cell strain in tissue culture. *Science*, 161(3839): 370-371.
- Betlazar, C., Middleton, R.J., Banati, R.B., & Liu, G.J. (2016). The impact of high and low dose ionising radiation on the central nervous system. *Redox Biology*, 9, 144-156.
- Bevelacqua, J.J. (2008). *Health Physics in the 21st Century*. Hoboken, NJ: John Wiley & Sons.
- Biedler, J.L., Helson, L., & Spengler, B.A. (1973). Morphology and growth, tumorigenicity, and cytogenetics of human neuroblastoma cells in continuous culture. *Cancer Research*, 33(11): 2643-2652.
- Biedler, J.L., Roffler-Tarlov, S., Schachner, M., & Freedman, L.S. (1978). Multiple neurotransmitter synthesis by human neuroblastoma cell lines and clones. *Cancer Research*, 38(11 Part 1): 3751-3757.
- Boado, R.J., Hui, E.K. W., Lu, J.Z., & Pardridge, W.M. (2010). Drug targeting of erythropoietin across the primate blood-brain barrier with an IgG molecular Trojan horse. *Journal of Pharmacology and Experimental Therapeutics*, 333(3): 961-969.
- Brenner, D.J., & Hall, E.J. (2007). Computed tomography—an increasing source of radiation exposure. *New England Journal of Medicine*, 357(22): 2277-2284.
- Brines, M. (2002). What evidence supports use of erythropoietin as a novel neurotherapeutic? *Oncology*, 16(9): 79-89.
- Brines, M., & Cerami, A. (2005). Emerging biological roles for erythropoietin in the nervous system. *Nature Reviews Neuroscience*, 6(6): 484-494.
- Brines, M.L., Ghezzi, P., Keenan, S., Agnello, D., De Lanerolle, N.C., Cerami, C., Itri, L.M. & Cerami, A. (2000). Erythropoietin crosses the blood-brain barrier to protect against experimental brain injury. *Proceedings of the National Academy of Sciences*, 97(19): 10526-10531.
- Bruno, C., & Czysz, P. A. (2009). *Future Spacecraft Propulsion Systems: Enabling Technologies for Space Exploration*. Berlin, Germany: Springer Science & Business Media.
- Buemi, M., Cavallaro E., Floccari F., Sturiale A., Aloisi C., Trimarchi M., Corica F., & Frisina N. (2003). The pleiotropic effects of erythropoietin in the central nervous system. *Journal of Neuropathology & Experimental Neurology*, 62(3): 228-236.
- Butler, J.M., Rapp, S.R., & Shaw, E.G. (2006). Managing the cognitive effects of brain tumor radiation therapy. *Current Treatment Options in Oncology*, 7(6): 517-523.

Butler, R.W., & Haser, J.K. (2006). Neurocognitive effects of treatment for childhood cancer. *Mental Retardation and Developmental Disabilities Research Reviews*, 12(3): 184-191.

Byts, N., & Sirén, A.L. (2009). Erythropoietin: a multimodal neuroprotective agent. *Experimental & Translational Stroke Medicine*, 1(1): 4.

Calabrese, V., Cornelius, C., Mancuso, C., Pennisi, G., Calafato, S., Bellia, F., Bates, T.E., Stella, A.M.G., Schapira, T., Kostova, A.T.D. & Rizzarelli, E. (2008). Cellular stress response: a novel target for chemoprevention and nutritional neuroprotection in aging, neurodegenerative disorders and longevity. *Neurochemical Research*, 33(12): 2444-2471.

Casadesus, G., Shukitt-Hale, B., Cantuti-Castelvetri, I., Rabin, B.M., & Joseph, J.A. (2004). The effects of heavy particle irradiation on exploration and response to environmental change. *Advances in Space Research*, 33(8): 1340-1346.

Casadesus, G., Shukitt-Hale, B., Stellwagen, H.M., Smith, M.A., Rabin, B.M., & Joseph, J.A. (2005). Hippocampal neurogenesis and PSA-NCAM expression following exposure to ⁵⁶Fe particles mimics that seen during aging in rats. *Experimental Gerontology*, 40(3): 249-254.

Central Brain Tumor Registry of the United States. (2014). 2014 CBTRUS Fact Sheet. Accessed March 16, 2016. <http://www.cbtrus.org/factsheet/factsheet.html>.

Chancellor, J.C., Scott, G.B., & Sutton, J.P. (2014). Space radiation: the number one risk to astronaut health beyond low earth orbit. *Life*, 4(3): 491-510.

Cherry, J.D., Liu, B., Frost, J.L., Lemere, C.A., Williams, J.P., Olschowka, J.A., & O'Banion, M.K. (2012). Galactic cosmic radiation leads to cognitive impairment and increased A β plaque accumulation in a mouse model of Alzheimer's disease. *PloS One*, 7(12): e53275.

Cheung, Y.T., Lau, W.K.W., Yu, M.S., Lai, C.S.W., Yeung, S.C., So, K.F., & Chang, R.C.C. (2009). Effects of all-trans-retinoic acid on human SH-SY5Y neuroblastoma as in vitro model in neurotoxicity research. *Neurotoxicology*, 30(1): 127-135.

Chopp, M., Chan, P.H., Hsu, C.Y., Cheung, M.E., & Jacobs, T.P. (1996). DNA damage and repair in central nervous system injury. *Stroke*, 27(3): 363-369.

Clagett-Dame, M., McNeill, E.M., & Muley, P.D. (2006). Role of all-trans retinoic acid in neurite outgrowth and axonal elongation. *Journal of Neurobiology*, 66(7): 739-756.

Constantinescu, R., Constantinescu, A.T., Reichmann, H., & Janetzky, B. (2007). Neuronal differentiation and long-term culture of the human neuroblastoma line SH-SY5Y. *Journal of Neural Transmission. Supplementum*, no. 72: 17-28.

Consumer Reports. (January 27, 2015). Dangers of CT scans and x-rays. Accessed December 21, 2015.

<http://www.consumerreports.org/cro/magazine/2015/01/the-surprising-dangers-of-ct-scans-and-x-rays/index.htm>.

Craven, P.A., & Rycroft, M.J. (1994). Fluxes of galactic iron nuclei and associated HZE secondaries, and resulting radiation doses, in the brain of an astronaut. *Advances in Space Research*, 14(10): 873-878.

Cucinotta, F.A. (2014). Space radiation risks for astronauts on multiple International Space Station missions. *PloS one*, 9(4): e96099.

Cucinotta, F.A., Alp, M., Sulzman, F.M., & Wang, M. (2014). Space radiation risks to the central nervous system. *Life Sciences in Space Research*, 2: 54-69.

Cucinotta, F.A., & Chappell, L.J. (2010). Non-targeted effects and the dose response for heavy ion tumor induction. *Mutation Research/Fundamental and Molecular Mechanisms of Mutagenesis*, 687(1): 49-53.

Cucinotta, F.A., & Durante, M. (2006). Cancer risk from exposure to galactic cosmic rays: implications for space exploration by human beings. *The Lancet Oncology*, 7(5): 431-435.

Cucinotta, F.A., Kim, M.H.Y., & Chappell, L.J. (2011). Space radiation cancer risk projections and uncertainties-2010. NASA Technical Paper 2011-216155.

Cucinotta, F.A., Kim, M.H.Y., Chappell, L.J., & Huff, J.L. (2013). How safe is safe enough? Radiation risk for a human mission to Mars. *PLoS One*, 8(10): e74988.

Cucinotta, F.A., Kim, M.H.Y., & Ren, L. (2006). Evaluating shielding effectiveness for reducing space radiation cancer risks. *Radiation Measurements*, 41(9): 1173-1185.

Cucinotta, F.A., Kim, M.H.Y., Willingham, V., & George, K.A. (2008). Physical and biological organ dosimetry analysis for international space station astronauts. *Radiation Research*, 170(1), 127-138.

Cucinotta, F.A., Schimmerling, W., Wilson, J.W., Peterson, L.E., Badhwar, G.D., Saganti, P.B., & Dicello, J.F. (2001). Space radiation cancer risks and uncertainties for Mars missions. *Radiation Research*, 156(5): 682-688.

Cucinotta, F.A., Wang, H., & Huff, J.L. (2012). Risk of acute or late central nervous system effects from radiation exposure. *Human Health and Performance Risks of Space Exploration Missions*. 191–212.

Curtis, S.B., & Letaw, J.R. (1989). Galactic cosmic rays and cell-hit frequencies outside the magnetosphere. *Advances in Space Research*, 9(10): 293-298.

Das, K.P., Freudenrich, T.M., & Mundy, W.R. (2004). Assessment of PC12 cell differentiation and neurite growth: a comparison of morphological and neurochemical measures. *Neurotoxicology and Teratology*, 26(3): 397-406.

Datta, K., Suman, S., Kallakury, B.V., & Fornace Jr, A.J. (2012). Exposure to heavy ion radiation induces persistent oxidative stress in mouse intestine. *PloS one*, 7(8): e42224.

de Almeida-Leite, C.M., & Arantes, R.M.E. (2010). Primary culture of glial cells from mouse sympathetic cervical ganglion: a valuable tool for studying glial cell biology. *Journal of Neuroscience Methods*, 194(1): 81-86.

Denisova, N.A., Shukitt-Hale, B., Rabin, B.M., & Joseph, J.A. (2002). Brain signaling and behavioral responses induced by exposure to ⁵⁶Fe-particle radiation. *Radiation Research*, 158(6): 725-734.

Dent, E.W., & Gertler, F.B. (2003). Cytoskeletal dynamics and transport in growth cone motility and axon guidance. *Neuron*, 40(2): 209-227.

Dent, E.W., Tang, F., & Kalil, K. (2003). Axon guidance by growth cones and branches: common cytoskeletal and signaling mechanisms. *The Neuroscientist*, 9(5): 343-353.

Desai, N., Davis, E., O'neill, P., Durante, M., Cucinotta, F.A., & Wu, H. (2005). Immunofluorescence detection of clustered γ -H2AX foci induced by HZE-particle radiation. *Radiation Research*, 164(4): 518-522.

Durante, M., & Cucinotta, F.A. (2008). Heavy ion carcinogenesis and human space exploration. *Nature Reviews Cancer*, 8(6): 465-472.

Dwane, S., Durack, E., & Kiely, P.A. (2013). Optimising parameters for the differentiation of SH-SY5Y cells to study cell adhesion and cell migration. *BMC Research Notes*, 6(1): 366.

Edsjö, A., Holmquist, L., & Pählman, S. (2007). Neuroblastoma as an experimental model for neuronal differentiation and hypoxia-induced tumor cell dedifferentiation. *Seminars in Cancer Biology*, 17(3): 248-256.

- Ehrenreich, H., Hasselblatt, M., Dembowski, C., Cepek, L., Lewczuk, P., Stiefel, M., Rustenbeck, H.H., Breiter, N., Jacob, S., Knerlich, F., & Bohn, M. (2002). Erythropoietin therapy for acute stroke is both safe and beneficial. *Molecular Medicine*, 8(8): 495.
- Encinas, M., Iglesias, M., Liu, Y., Wang, H., Muhaisen, A., Cena, V., Gallego, C. & Comella, J.X. (2000). Sequential treatment of SH-SY5Y cells with retinoic acid and brain-derived neurotrophic factor gives rise to fully differentiated, neurotrophic factor-dependent, human neuron-like cells. *Journal of Neurochemistry*, 75(3): 991-1003.
- Estable-Puig, J.F., de Estable, R.F., Tobias, C., & Haymaker, W. (1964). Degeneration and regeneration of myelinated fibers in the cerebral and cerebellar cortex following damage from ionizing particle radiation. *Acta Neuropathologica*, 4(2): 175-190.
- Geraldo, S., & Gordon-Weeks, P.R. (2009). Cytoskeletal dynamics in growth-cone steering. *Journal of Cell Science*, 122(20): 3595-3604.
- Giedzinski, E., Rola, R., Fike, J. R., & Limoli, C. L. (2005). Efficient production of reactive oxygen species in neural precursor cells after exposure to 250 MeV protons. *Radiation Research*, 164(4): 540-544.
- Gobbel, G. T., Bellinzona, M., Vogt, A.R., Gupta, N., Fike, J.R., & Chan, P.H. (1998). Response of postmitotic neurons to X-irradiation: implications for the role of DNA damage in neuronal apoptosis. *Journal of Neuroscience*, 18(1): 147-155.
- Goldberg, I.D., Bloomer, W.D., & Dawson, D.M. (1982). Nervous system toxic effects of cancer therapy. *Journal of the American Medical Association*, 247(10): 1437-1441.
- Goldberg, D.J., & Burmeister, D.W. (1986). Stages in axon formation: observations of growth of Aplysia axons in culture using video-enhanced contrast-differential interference contrast microscopy. *Journal of Cell Biology*, 103(5): 1921-1931.
- Grobben, B., De Deyn, P., & Slegers, H. (2002). Rat C6 glioma as experimental model system for the study of glioblastoma growth and invasion. *Cell and Tissue Research*, 310(3): 257-270.
- Hall, E.J., & Giaccia, A.J. (2006). *Radiobiology for the Radiologist*. Philadelphia, PA: Lippincott Williams & Wilkins.
- Hall E.J., & Giaccia, A.J. (2012). *Radiobiology for the Radiologist*. Philadelphia, PA: Lippincott Williams & Wilkins.
- Hanawalt, P.C., Gee, P., Ho, L., Hsu, R.K., & Kane, C.J. (1992). Genomic heterogeneity of DNA repair. *Annals of the New York Academy of Sciences*, 663(1): 17-25.

Hancock, M.K., Kopp, L., Kaur, N., & Hanson, B.J. (2015). A facile method for simultaneously measuring neuronal cell viability and neurite outgrowth. *Current Chemical Genomics and Translational Medicine*, 9: 6.

Harrill, J.A., Robinette, B.L., Freudenrich, T., & Mundy, W.R. (2013). Use of high content image analyses to detect chemical-mediated effects on neurite subpopulations in primary rat cortical neurons. *Neurotoxicology*, 34: 61-73.

Health and Safety Executive (HSE). (2015). Non-ionising radiation. Accessed April 19, 2015. <http://www.hse.gov.uk/radiation/nonionising/>.

Held, K.D. (2009). Effects of low fluences of radiations found in space on cellular systems. *International Journal of Radiation Biology*, 85(5): 379–390.

Hunt, W.A., Joseph, J.A., & Rabin, B.M. (1989). Behavioral and neurochemical abnormalities after exposure to low doses of high-energy iron particles. *Advances in Space Research*, 9(10): 333-336.

Hwang, S.Y., Jung, J.S., Kim, T.H., Lim, S.J., Oh, E.S., Kim, J.Y., Ji, K.A., Joe, E.H., Cho, K.H. and Han, I.O. (2006). Ionizing radiation induces astrocyte gliosis through microglia activation. *Neurobiology of Disease*, 21(3): 457-467.

International Agency for Research on Cancer (IARC) Working Group on the Evaluation of Carcinogenic Risks to Humans. (2002). Non-ionizing radiation, Part 1: Static and extremely low-frequency (ELF) electric and magnetic fields. *IARC Monographs on the Evaluation of Carcinogenic Risks to Humans*, 80: 1–395.

International Agency for Research on Cancer (IARC) Working Group on the Evaluation of Carcinogenic Risks to Humans. (2013). Non-ionizing radiation, Part 2: Radiofrequency electromagnetic fields. *IARC Monographs on the Evaluation of Carcinogenic Risks to Humans*, 102(Pt 2): 1–460.

International Commission on Non-Ionizing Radiation Protection. (2015). Accessed April 21, 2016. <http://www.icnirp.org/en/home/index.html>.

Iwata-Ichikawa, E., Kondo, Y., Miyazaki, I., Asanuma, M., & Ogawa, N. (1999). Glial cells protect neurons against oxidative stress via transcriptional up-regulation of the glutathione synthesis. *Journal of Neurochemistry*, 72(6): 2334-2344.

Jalink, K., van Corven, E.J., Hengeveld, T., Morii, N., Narumiya, S., & Moolenaar, W.H. (1994). Inhibition of lysophosphatidate- and thrombin-induced neurite retraction and neuronal cell rounding by ADP-ribosylation of the small GTP-binding protein Rho. *The Journal of Cell Biology*, 126(3): 801-810.

John Hopkins Medicine. (2016). Treatment for Gliomas. Accessed October 9, 2016. http://www.hopkinsmedicine.org/neurology_neurosurgery/centers_clinics/brain_tumor/center/glioma/treatment.html.

Joseph, J.A., & Cutler, R.C. (1994). The role of oxidative stress in signal transduction changes and cell loss in senescence. *Annals of the New York Academy of Sciences*, 738(1): 37-43.

Joseph, J.A., Hunt, W.A., Rabin, B.M., & Dalton, T.K. (1992). Possible "accelerated striatal aging" induced by ⁵⁶Fe heavy-particle irradiation: Implications for manned space flights. *Radiation Research*, 130(1): 88-93.

Joseph, J.A., Hunt, W.A., Rabin, B.M., Dalton, T.K., & Harris, A.H. (1993). Deficits in the sensitivity of striatal muscarinic receptors induced by heavy-particle irradiation: Further "age-radiation" parallels. *Radiation Research*, 135(2): 257-261.

Juul, S.E., Anderson, D.K., Li, Y., & Christensen, R.D. (1998). Erythropoietin and erythropoietin receptor in the developing human central nervous system. *Pediatric Research*, 43(1): 40-49.

Kandel, E.R., Schwartz J.H., & Jessell, T.M. (2000). *Principles of Neural Science*. (Vol. 4). New York City, NY: McGraw-Hill.

Kann, O., & Kovács, R. (2007). Mitochondria and neuronal activity. *American Journal of Physiology-Cell Physiology*, 292(2): C641-C657.

Karran, E., Mercken, M., & De Strooper, B. (2011). The amyloid cascade hypothesis for Alzheimer's disease: an appraisal for the development of therapeutics. *Nature Reviews Drug Discovery*, 10(9): 698-712.

Kelsey, N.A., Wilkins, H.M., & Linseman, D.A. (2010). Nutraceutical antioxidants as novel neuroprotective agents. *Molecules*, 15(11): 7792-7814.

Kennedy, A.R. (2014). Biological effects of space radiation and development of effective countermeasures. *Life Sciences in Space Research*, 1: 10-43.

Keswani, S.C., Buldanlioglu, U., Fischer, A., Reed, N., Polley, M., Liang, H., Zhou, C., Jack, C., Leitz, G.J., & Hoke, A., (2004). A novel endogenous erythropoietin mediated pathway prevents axonal degeneration. *Annals of Neurology*, 56(6): 815-826.

Kevenaar, J.T., & Hoogenraad, C.C. (2015). The axonal cytoskeleton: from organization to function. *Frontiers in Molecular Neuroscience*, 8: 44.

Kim, M.H.Y., Cucinotta, F.A., Nounu, H.N., Zeitlin, C., Hassler, D.M., Rafkin, S.C., Wimmer-Schweingruber, R.F., Ehresmann, B., Brinza, D.E., Böttcher, S. & Böhm, E. (2014). Comparison of Martian surface ionizing radiation measurements from MSL-

RAD with Badhwar-O'Neill 2011/HZETRN model calculations. *Journal of Geophysical Research: Planets*, 119(6): 1311-1321.

Kirkpatrick, L.L., & Brady, S.T. (1999). Molecular components of the neuronal cytoskeleton. *Basic Neurochemistry: Molecular, Cellular and Medical Aspects*. Philadelphia, PA: Lippincott-Raven.

Korecka, J.A., van Kesteren, R.E., Blaas, E., Spitzer, S.O., Kamstra, J.H., Smit, A.B., Swaab, D.F., Verhaagen, J. and Bossers, K. (2013). Phenotypic characterization of retinoic acid differentiated SH-SY5Y cells by transcriptional profiling. *PloS one*, 8(5): e63862.

Kovalevich, J., & Langford, D. (2013). Considerations for the use of SH-SY5Y neuroblastoma cells in neurobiology. *Neuronal Cell Culture: Methods and Protocols*, 9-21.

Kudo, S., Suzuki, Y., Noda, S.E., Mizui, T., Shirai, K., Okamoto, M., Kaminuma, T., Yoshida, Y., Shirao, T. & Nakano, T. (2014). Comparison of the radiosensitivities of neurons and glial cells derived from the same rat brain. *Experimental and Therapeutic Medicine*, 8(3): 754-758.

Kuwahara, Y., Oikawa, T., Ochiai, Y., Roudkenar, M.H., Fukumoto, M., Shimura, T., Ohtake, Y., Ohkubo, Y., Mori, S. and Uchiyama, Y. (2011). Enhancement of autophagy is a potential modality for tumors refractory to radiotherapy. *Cell Death & Disease*, 2(6): e177.

Kyrkanides, S., Moore, A.H., Olschowka, J.A., Daeschner, J.C., Williams, J.P., Hansen, J.T., & O'Banion, M.K. (2002). Cyclooxygenase-2 modulates brain inflammation-related gene expression in central nervous system radiation injury. *Molecular Brain Research*, 104(2): 159-169.

Lee, C.I., Haims, A.H., Monico, E.P., Brink, J.A., & Forman, H.P. (2004). Diagnostic CT scans: Assessment of patient, physician, and radiologist awareness of radiation dose and possible risks 1. *Radiology*, 231(2): 393-398.

Lee, J., Koo, N., & Min, D.B. (2004). Reactive oxygen species, aging, and antioxidative nutraceuticals. *Comprehensive Reviews in Food Science and Food Safety*, 3(1): 21-33.

Letaw, J.R., Silberberg, R., & Tsao, C.H. (1989). Radiation hazards on space missions outside the magnetosphere. *Advances in Space Research*, 9(10): 285-291.

Li, Y., Lu, Z.Y., Ogle, M., & Wei, L. (2007). Erythropoietin prevents blood brain barrier damage induced by focal cerebral ischemia in mice. *Neurochemical Research*, 32(12): 2132-2141.

- Liao, A.C., Craver, B.M., Tseng, B.P., Tran, K.K., Parihar, V.K., Acharya, M.M., & Limoli, C.L. (2013). Mitochondrial-targeted human catalase affords neuroprotection from proton irradiation. *Radiation Research*, 180(1): 1-6.
- Lin, M.T., & Beal, M.F. (2006). Mitochondrial dysfunction and oxidative stress in neurodegenerative diseases. *Nature*, 443(7113): 787-795.
- Linseman, D.A. (2009). Targeting oxidative stress for neuroprotection. *Antioxidants & Redox Signaling*, 11(3): 421-424.
- Little, M.P., Tawn, E.J., Tzoulaki, I., Wakeford, R., Hildebrandt, G., Paris, F., Tapio, S. & Elliott, P. (2010). Review and meta-analysis of epidemiological associations between low/moderate doses of ionizing radiation and circulatory disease risks, and their possible mechanisms. *Radiation and Environmental Biophysics*, 49(2): 139-153.
- Love, S. (2006). Demyelinating diseases. *Journal of Clinical Pathology*, 59(11): 1151-1159.
- Lowery, L.A., & Van Vactor, D. (2009). The trip of the tip: understanding the growth cone machinery. *Nature Reviews Molecular Cell Biology*, 10(5): 332-343.
- Lykissas, M.G., Korompilias, A.V., Vekris, M.D., Mitsionis, G.I., Sakellariou, E., & Beris, A.E. (2007). The role of erythropoietin in central and peripheral nerve injury. *Clinical Neurology and Neurosurgery*, 109(8): 639-644.
- Maris, J.M. (2010). Recent advances in neuroblastoma. *New England Journal of Medicine*, 362(23): 2202-2211.
- Martin, I., & Grotewiel, M.S. (2006). Oxidative damage and age-related functional declines. *Mechanisms of Ageing and Development*, 127(5): 411-423.
- Martínez-Estrada, O.M., Rodríguez-Millán, E., González-de Vicente, E., Reina, M., Vilaró, S., & Fabre, M. (2003). Erythropoietin protects the in vitro blood-brain barrier against VEGF-induced permeability. *European Journal of Neuroscience*, 18(9): 2538-2544.
- McCarty, M.F. (2006). Toward prevention of Alzheimers disease-potential nutraceutical strategies for suppressing the production of amyloid beta peptides. *Medical Hypotheses*, 67(4): 682-697.
- McDonald, W.I., & Sears, T.A. (1969). Effect of demyelination on conduction in the central nervous system. *Nature*, 221(5176): 182-183.
- McKenna-Lawlor, S., Gonçalves, P., Keating, A., Reitz, G., & Matthiä, D. (2012). Overview of energetic particle hazards during prospective manned missions to Mars. *Planetary and Space Science*, 63: 123-132.

- Meikrantz, W., & Schlegel, R. (1995). Apoptosis and the cell cycle. *Journal of Cellular Biochemistry*, 58(2): 160-174.
- Memon, S.A., Laghari N.A., Mangi F.H., Ahmad F., Hussain M.M., Paliyo S., Jhatyal N., & Adeel A. (2015). Analysis and verification of percent depth dose and tissue maximum ratio for Co-60 gamma ray beam. *World Applied Sciences Journal*, 33(1): 109-113.
- Meraz-Ríos, M.A., Toral-Rios, D., Franco-Bocanegra, D., Villeda-Hernández, J., & Campos-Peña, V. (2013). Inflammatory process in Alzheimer's Disease. *Frontiers in Integrative Neuroscience*, 7.
- Mercola, Joseph. (2016). The ultimate guide to antioxidants. Accessed May 5, 2016. <http://articles.mercola.com/antioxidants.aspx>.
- Mizumatsu, S., Monje, M.L., Morhardt, D.R., Rola, R., Palmer, T.D., & Fike, J.R. (2003). Extreme sensitivity of adult neurogenesis to low doses of X-irradiation. *Cancer Research*, 63(14): 4021-4027.
- Monje, M.L., Mizumatsu, S., Fike, J.R., & Palmer, T.D. (2002). Irradiation induces neural precursor-cell dysfunction. *Nature Medicine*, 8(9): 955-962.
- Moore, A.H., Olschowka, J.A., Williams, J.P., Okunieff, P., & O'Banion, M.K. (2005). Regulation of prostaglandin E 2 synthesis after brain irradiation. *International Journal of Radiation Oncology, Biology, Physics*, 62(1): 267-272.
- Morgan, W.F., Day, J.P., Kaplan, M.I., McGhee, E.M., & Limoli, C.L. (1996). Genomic instability induced by ionizing radiation. *Radiation Research*, 146(3): 247-258.
- Morgan, W.F., & Sowa, M.B. (2007). Non-targeted bystander effects induced by ionizing radiation. *Mutation Research/Fundamental and Molecular Mechanisms of Mutagenesis*, 616(1): 159-164.
- Morishita, E., Masuda, S., Nagao, M., Yasuda, Y., & Sasaki, R. (1996). Erythropoietin receptor is expressed in rat hippocampal and cerebral cortical neurons, and erythropoietin prevents in vitro glutamate-induced neuronal death. *Neuroscience*, 76(1): 105-116.
- Mukherjee, B., Camacho, C.V., Tomimatsu, N., Miller, J., & Burma, S. (2008). Modulation of the DNA-damage response to HZE particles by shielding. *DNA Repair*, 7(10): 1717-1730.
- National Aeronautics and Space Administration. (October, 2002). Understanding space radiation. Accessed April 14, 2015. <http://spaceflight.nasa.gov/spaceneeds/factsheets/pdfs/radiation.pdf>.

National Aeronautics and Space Administration. (December 12, 2008). Modeling radiation exposure for pilots, crew and passengers on commercial flights. Accessed April 14, 2015. <http://www.nasa.gov/topics/earth/features/AGU-NAIRAS.html>.

National Council on Radiation Protection and Measurements (NCRP). (2006). *Information needed to make radiation protection recommendations for space missions beyond low-Earth orbit: Recommendations of the National Council on Radiation Protection and Measurements*. NCRP Report No. 153. Bethesda, MD: National Council on Radiation Protection and Measurements.

National Institutes of Health, & National Cancer Institute. (2015). Magnetic field exposure and cancer. Accessed May 1, 2015. <http://www.cancer.gov/cancertopics/causes-prevention/risk/radiation/magnetic-fields-fact-sheet>.

National Institute for Occupational Safety and Health (NIOSH). (April 24, 2015). Aircrew safety & health. Centers for Disease Control and Prevention (CDC). Accessed April 14, 2016. <http://www.cdc.gov/niosh/topics/aircrew/cosmicionizingradiation.html>.

National Research Council. (1990). *Health effects of exposure to low levels of ionizing radiation: BEIR V* (Vol. 5). Washington, D.C.: National Academies Press.

National Research Council. (1997). *Space Studies Board Annual Report 1996*. Washington, D.C.: National Academies Press.

National Research Council. (2000). *Radiation and the International Space Station*. Washington, D.C.: National Academies Press.

National Research Council. (2006). *Health Risks from Exposure to Low Levels of Ionizing Radiation: BEIR VII Phase 2*. Washington, D.C.: National Academies Press.

Nicolini, G., Miloso, M., Zoia, C., Di Silvestro, A., Cavaletti, G., & Tredici, G. (1997). Retinoic acid differentiated SH-SY5Y human neuroblastoma cells: an in vitro model to assess drug neurotoxicity. *Anticancer Research*, 18(4A): 2477-2481.

Noctor, S.C., Flint, A.C., Weissman, T.A., Dammerman, R.S., & Kriegstein, A.R. (2001). Neurons derived from radial glial cells establish radial units in neocortex. *Nature*, 409(6821): 714-720.

Nunomura, A., Perry, G., Aliev, G., Hirai, K., Takeda, A., Balraj, E.K., Jones, P.K., Ghanbari, H., Wataya, T., Shimohama, S. & Chiba, S. 2001. Oxidative damage is the earliest event in Alzheimer disease. *Journal of Neuropathology & Experimental Neurology*, 60(8): 759-767.

- Nunomura, A., Perry, G., Pappolla, M.A., Wade, R., Hirai, K., Chiba, S., & Smith, M.A. (1999). RNA oxidation is a prominent feature of vulnerable neurons in Alzheimer's disease. *Journal of Neuroscience*, *19*(6): 1959-1964.
- Packer, L., Tritschler, H. J., & Wessel, K. (1997). Neuroprotection by the metabolic antioxidant α -lipoic acid. *Free Radical Biology and Medicine*, *22*(1): 359-378.
- Påhlman, S., Odelstad, L., Larsson, E., Grotte, G., & Nilsson, K. (1981). Phenotypic changes of human neuroblastoma cells in culture induced by 12-O-tetradecanoylphorbol-13-acetate. *International Journal of Cancer*, *28*(5): 583-589.
- Park, R. (2001). Cellular telephones and cancer: How should science respond? *Journal of the National Cancer Institute*, *93*(3): 166-67.
- Purves, D., Augustine G.J., Fitzpatrick D., Katz L.C., LaMantia A-S., McNamara J.O., & Williams S.M. (2001). *Neuroglial Cells*. Sunderland, MA: Sinauer Associates.
- Rabin, B.M., Hunt, W.A., & Joseph, J.A. (1989). An assessment of the behavioral toxicity of high-energy iron particles compared to other qualities of radiation. *Radiation Research*, *119*(1): 113-122.
- Rabin, B.M., Hunt, W.A., Joseph, J.A., Dalton, T.K., & Kandasamy, S.B. (1991). Relationship between linear energy transfer and behavioral toxicity in rats following exposure to protons and heavy particles. *Radiation Research*, *128*(2): 216-221.
- Rabin, B.M., Joseph, J.A., Hunt, W.A., Dalton, T.B., Kandasamy, S.B., Harris, A.H., & Ludewig, B. (1994). Behavioral endpoints for radiation injury. *Advances in Space Research*, *14*(10): 457-466.
- Rabin, B.M., Joseph, J.A., & Shukitt-Hale, B. (2003). Long-term changes in amphetamine-induced reinforcement and aversion in rats following exposure to ^{56}Fe particle. *Advances in Space Research*, *31*(1): 127-133.
- Rabin, B.M., Joseph, J.A., & Shukitt-Hale, B. (2005). Effects of age and diet on the heavy particle-induced disruption of operant responding produced by a ground-based model for exposure to cosmic rays. *Brain Research*, *1036*(1): 122-129.
- Rabin, B. M., Joseph, J. A., Shukitt-Hale, B., & McEwen, J. (2000). Effects of exposure to heavy particles on a behavior mediated by the dopaminergic system. *Advances in Space Research*, *25*(10): 2065-2074.
- Radio, N.M., & Mundy, W.R. (2008). Developmental neurotoxicity testing in vitro: models for assessing chemical effects on neurite outgrowth. *Neurotoxicology*, *29*(3): 361-376.

Raff, M.C., Fields, K.L., Hakomori, S.I., Mirsky, R., Pruss, R.M., & Winter, J. (1979). Cell-type-specific markers for distinguishing and studying neurons and the major classes of glial cells in culture. *Brain Research*, 174(2): 283-308.

Rask, J., Vercoutere, W., Navarro, B.J., & Krause, A. (2007). Space faring: The radiation challenge: An interdisciplinary guide on radiation biology for grades 9 through 12, Module 3: Radiation countermeasures. NASA Educational Product EP-2008-08-118-MSFC.

Reske-Nielsen E., Oster S., & Reintoft I. (1987). Astrocytes in the prenatal central nervous system. *APMIS*, 95(6): 339-346.

Rinne, M.L., Lee E.Q., & Wen P.Y. 2012. Central Nervous System Complications of Cancer Therapy. *The Journal of Supportive Oncology*, 10(4): 133-41.

Robb, M. (2004). Like one hundred x-rays? Study suggests many referring physicians don't grasp or explain to patients the radiation exposure involved with CT. *Radiology Today*, 22-24.

Rola, R., Sarkissian, V., Obenaus, A., Nelson, G.A., Otsuka, S., Limoli, C.L., & Fike, J.R. (2005). High-LET radiation induces inflammation and persistent changes in markers of hippocampal neurogenesis. *Radiation Research*, 164(4): 556-560.

Ross, R.A., Spengler, B.A., & Biedler, J.L. (1983). Coordinate morphological and biochemical interconversion of human neuroblastoma cells. *Journal of the National Cancer Institute*, 71(4): 741-747.

Saenko, Y., Cieslar-Pobuda, A., Skonieczna, M., & Rzeszowska-Wolny, J. (2013). Changes of reactive oxygen and nitrogen species and mitochondrial functioning in human K562 and HL60 cells exposed to ionizing radiation. *Radiation Research*, 180(4): 360-366.

Sagara, J.I., Miura, K., & Bannai, S. (1993). Maintenance of neuronal glutathione by glial cells. *Journal of Neurochemistry*, 61(5): 1672-1676.

Sakanaka, M., Wen, T.C., Matsuda, S., Masuda, S., Morishita, E., Nagao, M., & Sasaki, R. (1998). In vivo evidence that erythropoietin protects neurons from ischemic damage. *Proceedings of the National Academy of Sciences*, 95(8): 4635-4640.

Samari, N., Saint-Georges, D., Pani, G., Baatout, S., Leyns, L., & Benotmane, M.A. (2013). Non-conventional apoptotic response to ionising radiation mediated by N-methyl D-aspartate receptors in immature neuronal cells. *International Journal of Molecular Medicine*, 31(3): 516-524.

Samson, K. (2008). Study warns of increased radiation risk from excessive CT scans. *Neurology Today*, 8(2): 7-8.

- Schaffer, S., Asseburg, H., Kuntz, S., Muller, W.E., & Eckert, G.P. (2012). Effects of polyphenols on brain ageing and Alzheimer's disease: focus on mitochondria. *Molecular Neurobiology*, 46(1): 161-178.
- Schimmerling, W., Cucinotta, F.A., & Wilson, J.W. (2003). Radiation risk and human space exploration. *Advances in Space Research*, 31(1): 27-34.
- Schultheiss, T.E., Kun, L.E., Ang, K.K., & Stephens, L.C. (1995). Radiation response of the central nervous system. *International Journal of Radiation Oncology, Biology, Physics*, 31(5): 1093-1112.
- Setlow, R.B. (2003). The hazards of space travel. *EMBO Reports*, 4(11): 1013-1016.
- Shea, M.A. (2011). Solar particle events. In *Encyclopedia of Astrobiology*, 1527-1528. Berlin, Germany: Springer Berlin Heidelberg.
- Shukitt-Hale, B., Casadesus, G., McEwen, J.J., Rabin, B.M., & Joseph, J.A. (2000). Spatial learning and memory deficits induced by exposure to iron-56-particle radiation. *Radiation Research*, 154(1): 28-33.
- Simonsen, L.C., Wilson, J.W., Kim, M.H., & Cucinotta, F.A. (2000). Radiation exposure for human Mars exploration. *Health Physics*, 79(5): 515-525.
- Smith-Bindman, R., Miglioretti, D.L., & Larson, E.B. (2008). Rising use of diagnostic medical imaging in a large integrated health system. *Health Affairs*, 27(6): 1491-1502.
- Song, S.K., Yoshino, J., Le, T.Q., Lin, S.J., Sun, S.W., Cross, A.H., & Armstrong, R.C. (2005). Demyelination increases radial diffusivity in corpus callosum of mouse brain. *NeuroImage*, 26(1): 132-140.
- Sowa Resat, M.B., & Morgan, W.F. (2004). Radiation-induced genomic instability: A role for secreted soluble factors in communicating the radiation response to non-irradiated cells. *Journal of Cellular Biochemistry*, 92(5): 1013-1019.
- Space Radiation Analysis Group, NASA. (Updated June 10, 2016). What is space radiation? Accessed April 12, 2016.
<https://srag.jsc.nasa.gov/SpaceRadiation/What/What.cfm>
- Sridharan, D.M., Asaithamby, A., Bailey, S.M., Costes, S.V., Doetsch, P.W., Dynan, W.S., Kronenberg, A., Rithidech, K.N., Saha, J., Snijders, A.M. & Werner, E. (2015). Understanding cancer development processes after HZE-particle exposure: roles of ROS, DNA damage repair and inflammation. *Radiation Research*, 183(1): 1-26.
- Stein, T. P. (2002). Space flight and oxidative stress. *Nutrition*, 18(10): 867-871.

- Stickel, S., Gomes, N., & Su, T.T. (2014). The role of translational regulation in survival after radiation damage; an opportunity for proteomics analysis. *Proteomes*, 2(2): 272-290.
- Suman, S., Rodriguez, O.C., Winters, T.A., Fornace Jr, A.J., Albanese, C., & Datta, K. (2013). Therapeutic and space radiation exposure of mouse brain causes impaired DNA repair response and premature senescence by chronic oxidant production. *Aging*, 5(8): 607.
- Sun, A.M., Li, C.G., Han, Y.Q., Liu, Q.L., Xia, Q., & Yuan, Y.W. (2013). X-ray irradiation promotes apoptosis of hippocampal neurons through up-regulation of Cdk5 and p25. *Cancer Cell International*, 13(1): 47.
- Tofilon, P.J., & Fike, J.R. (2000). The radioresponse of the central nervous system: a dynamic process. *Radiation Research*, 153(4): 357-370.
- Tong, J.X., Vogelbaum, M.A., Drzymala, R.E., & Rich, K.M. (1997). Radiation-induced apoptosis in dorsal root ganglion neurons. *Journal of Neurocytology*, 26(11): 771-777.
- Townsend, L.W., Cucinotta, F.A., & Wilson, J.W. (1992). Interplanetary crew exposure estimates for galactic cosmic rays. *Radiation Research*, 129(1): 48-52.
- Townsend, L.W., Wilson, J.W., Shinn, J.L., & Curtis, S.B. (1992). Human exposure to large solar particle events in space. *Advances in Space Research*, 12(2-3): 339-348.
- United States Nuclear Regulatory Commission. (n.d.). Biological Effects of Radiation. Accessed April 14, 2015. <http://www.nrc.gov/reading-rm/basic-ref/teachers/09.pdf>.
- United States Nuclear Regulatory Commission. (n.d.). Doses in our daily lives. Accessed December 21, 2015. <http://www.nrc.gov/about-nrc/radiation/around-us/doses-daily-lives.html>.
- University of Maryland Medical Center. (2014). Alpha-Lipoic Acid. Accessed May 5, 2015. <http://umm.edu/health/medical/altmed/supplement/alphalipoic-acid>.
- Vitriol, E.A., & Zheng, J.Q. (2012). Growth cone travel in space and time: the cellular ensemble of cytoskeleton, adhesion, and membrane. *Neuron*, 73(6): 1068-1081.
- Voress, M. (2007). The increasing use of CT and its risks. *Radiologic Technology*, 79(2): 186-190.
- Ward, J.F. (1988). DNA damage produced by ionizing radiation in mammalian cells: Identities, mechanisms of formation, and reparability. *Progress in Nucleic Acid Research and Molecular Biology*, 35: 95-125.

Wilson, J.W. (2000). Overview of radiation environments and human exposures. *Health Physics*, 79(5): 470-494.

Wu, H., Huff, J.L., Casey, R., Kim, M.H., & Cucinotta, F.A. (2009). Risk of acute radiation syndromes due to solar particle events. *The Human Health and Performance Risks for Space Explorations*. Houston, Texas: NASA Human Research Program, 171-190.

Yamamori, T., Yasui, H., Yamazumi, M., Wada, Y., Nakamura, Y., Nakamura, H., & Inanami, O. (2012). Ionizing radiation induces mitochondrial reactive oxygen species production accompanied by upregulation of mitochondrial electron transport chain function and mitochondrial content under control of the cell cycle checkpoint. *Free Radical Biology and Medicine*, 53(2): 260-270.

Zeitlin, C., Hassler, D.M., Cucinotta, F.A., Ehresmann, B., Wimmer-Schweingruber, R.F., Brinza, D.E., Kang, S., Weigle, G., Böttcher, S., Böhm, E., & Burmeister, S. (2013). Measurements of energetic particle radiation in transit to Mars on the Mars Science Laboratory. *Science*, 340(6136): 1080-1084.

Zhang, F., Xing, J., Liou, A.K.F., Wang, S., Gan, Y., Luo, Y., Ji, X., Stetler, R.A., Chen, J., & Cao, G. (2010). Enhanced delivery of erythropoietin across the blood-brain barrier for neuroprotection against ischemic neuronal injury. *Translational Stroke Research*, 1(2): 113-121.

Zhou, X.D., Wang, X.Y., Qu, F.J., Zhong, Y.H., Lu, X.D., Zhao, P., Wang, D.H., Huang, Q.B., Zhang, L. & Li, X.G. (2009). Detection of cancer stem cells from the C6 glioma cell line. *Journal of International Medical Research*, 37(2): 503-510.